# *A Preconditioner for Fictitious Domain Formulations of Elliptic PDEs on Uncertain Parameterized Domains*

Powell, Catherine E. and Gordon, Andrew D.

2013

MIMS EPrint: **2013.31**

Manchester Institute for Mathematical Sciences
School of Mathematics

The University of Manchester

Reports available from: http://eprints.maths.manchester.ac.uk/
And by contacting: The MIMS Secretary
School of Mathematics
The University of Manchester
Manchester, M13 9PL, UK

ISSN 1749-9097

# A PRECONDITIONER FOR FICTITIOUS DOMAIN FORMULATIONS OF ELLIPTIC PDES ON UNCERTAIN PARAMETERIZED DOMAINS*

ANDREW GORDON AND CATHERINE E. POWELL ‡

**Abstract.** We consider the numerical solution of elliptic boundary-value problems on uncertain two-dimensional domains via the fictitious domain method. This leads to variational problems of saddle point form. Working under the standard assumption that the domain can be described by a finite number of independent random variables, discretization is achieved by a stochastic collocation mixed finite element method. We focus on the efficient iterative solution of the resulting sequence of indefinite linear systems and introduce a novel and efficient preconditioner for use with the minimal residual method. The challenging task is to construct a matrix that provides a robust approximation to a discrete representation of a trace space norm on a parameterized boundary.

**Key words.** mixed finite elements, saddle point problems, stochastic collocation, random domains, algebraic multigrid, preconditioning.

**AMS subject classifications.** 35R60, 65C20, 65N30, 65NF08, 65F10

**1. Introduction.** Numerical methods for solving partial differential equations (PDEs) with uncertain (or random) data is currently a very active research area. In particular, there is now a vast literature treating elliptic PDEs with uncertain coefficients (see e.g., [4], [24], [23], [5], [21], [10], [13], [17],[12]). Discretization schemes (e.g., Monte Carlo, stochastic Galerkin, stochastic collocation), error bounds and iterative solvers for such problems have been extensively studied. On the other hand, PDEs posed on domains with uncertain *geometry* or more precisely, domains described by uncertain parameters (see [3], [9], [19] and [30]), have received less attention. Solutions to such problems often have low regularity and existing literature focuses on the challenging question of well-posedness, regularity results and a priori error estimates. Armed with such analysis and a tried and tested discretization scheme for deterministic PDEs, we focus here on efficient linear algebra.

We examine second-order elliptic PDEs on uncertain domains $D \subset \mathbb{R}^2$. To account for uncertainty, we take a probabilistic approach and treat $D$ as a function of $\omega \in \Omega$, where $\Omega$ is an abstract sample space. To that end, let $(\Omega, \mathcal{F}, \mathbb{P})$ be a probability space, consisting of the sample space $\Omega$, a $\sigma$-algebra $\mathcal{F}$ and probability measure $\mathbb{P}$. For each $\omega \in \Omega$, $D(\omega)$ is a realization of $D$ with boundary $\partial D(\omega)$ and we assume $D(\omega)$ is a bounded polygon $\mathbb{P}-$a.s. (with probability one). Now, let $D : \Omega \to \mathcal{B}(\mathbb{R}^2)$, where $\mathcal{B}(\mathbb{R}^2)$ is the Borel $\sigma$-algebra on $\mathbb{R}^2$ and assume the data $a, f : \widehat{D} \to \mathbb{R}$ where

$$\widehat{D} := \bigcup_{\omega \in \Omega} D(\omega). \tag{1.1}$$

We want to find $p : \left\{(\boldsymbol{x}, \omega) : \omega \in \Omega, \boldsymbol{x} \in \overline{D(\omega)}\right\} \to \mathbb{R}$ such that $\mathbb{P}-$a.s.,

$$-\nabla \cdot (a(\boldsymbol{x}) \nabla p(\boldsymbol{x}, \omega)) = f(\boldsymbol{x}) \qquad \text{in } D(\omega), \tag{1.2}$$

$$p(\boldsymbol{x}, \omega) = 0 \qquad \text{on } \partial D(\omega). \tag{1.3}$$

*Supported by the EPSRC under grant no. EP/H021205/1.

‡School of Mathematics, University of Manchester, Oxford Road, Manchester M13 9PL, United Kingdom. (c.powell@manchester.ac.uk).

For simplicity, we focus on homogeneous Dirichlet boundary conditions, as in [30] and [9]; Neumann boundary conditions are considered in [19]. There are many reasons why the domain for the model problem (1.2)–(1.3) could be uncertain. It may correspond to an object that is inaccessible (such as a subterranean layer of rock in a potential flow simulation) or to an object that is subject to manufacturing inaccuracies (such as a component of an engine in a steady-state heat diffusion simulation).

One possibility is to transform (1.2)–(1.3) into a boundary-value problem (BVP) on a fixed domain $E \subset \mathbb{R}^2$. Suppose there exists an invertible mapping $\boldsymbol{\eta} = \boldsymbol{\eta}(\boldsymbol{x}, \omega)$ with inverse $\boldsymbol{x} = \boldsymbol{x}(\boldsymbol{\eta}, \omega)$, that transforms $D(\omega)$ into $E$. That is, for almost every $\omega \in \Omega$, $\boldsymbol{x} \in D(\omega)$ gives $\boldsymbol{\eta} \in E$ and $\boldsymbol{\eta}(D(\omega), \omega) = E$. By applying a change of variable, (1.2)–(1.3) can be transformed into a new BVP on $E$ with random data $\widehat{a}(\boldsymbol{\eta}, \omega)$, $\widehat{f}(\boldsymbol{\eta}, \omega)$. Details about how to construct such a mapping can be found in [30].

Of course, we could also solve (1.2)–(1.3) directly by a Monte Carlo method. That is, generate realizations $D(\omega)$ of $D$ and solve the resulting deterministic BVPs using e.g., finite elements. A serious disadvantage is that for each $D(\omega)$, re-meshing is required and a new finite element stiffness matrix has to be formed. A different approach, based on the fictitious domain method (FDM) [14, 15] is taken in [9]. Here, (1.2)–(1.3) is solved on a larger fixed domain $E$, in the original co-ordinate system, and the boundary conditions are enforced weakly on $\partial D$. This yields a saddle point problem with deterministic coefficients. When sampling is applied, only one stiffness matrix is required on $E$ and only the boundary $\partial D$ needs to be re-meshed. Hence, we follow [9] and use the FDM strategy.

In Section 2, we briefly review the FDM for solving PDEs on fixed, certain domains. We return to the stochastic problem (1.2)–(1.3) in Section 3 and assume that $D(\omega)$ can be described by a finite number of random variables $\xi_k : \Omega \to \mathbb{R}$. In this work, we assume the $\xi_k$ are bounded. We then combine the FDM with a stochastic collocation mixed finite element method (SCMFEM) (see [25], [29]). The main contribution of our work is presented in Section 4, where we consider the efficient numerical solution of the sequences of linear systems generated by the combined FDM-SCMFEM scheme. In particular, we introduce a novel preconditioner for use with minimal residual (MINRES) iteration. Numerical results are also presented to investigate robustness of the suggested solver with respect to the discretization parameters and the statistical parameters describing the uncertainty in the domain geometry. To conclude this introduction, we recall some standard definitions and results that will be needed in the sequel.

**1.1. Trace spaces and norms.** Consider a bounded set $E \subset \mathbb{R}^2$ with boundary $\partial E$ and let $H^1(E)$ denote the Hilbert space of $L^2(E)$ functions with weak first derivatives in $L^2(E)$. If $\partial E$ is sufficiently smooth then it is well known (e.g., see [2, Section 7.3.4]) that there exists a bounded operator $\tau : H^1(E) \to L^2(\partial E)$, called a trace operator, that satisfies $\tau(v) = v|_{\partial E}$ for all $v \in H^1(E) \cap C^1(\overline{E})$. The range of $\tau$ is not the whole of $L^2(\partial E)$ but the so-called trace space $H^{1/2}(\partial E)$. We next recall that $H^1_0(E) = \left\{ v \in H^1(E) \,:\, \tau(v) = 0 \right\}$, the set of $H^1(E)$ functions that are zero, in the sense of trace, on $\partial E$. For $v \in H^1_0(E)$, we define

$$\|v\|_{H^1_0(E)} := \|\nabla v\|_{L^2(E)}, \qquad \|v\|_{H^1(E)} := \left( \|v\|^2_{L^2(E)} + \|v\|^2_{H^1_0(E)} \right)^{1/2},$$

and, denoting the Poincaré constant for $E$ by $K_E$, we recall the norm equivalence,

$$\|v\|_{H^1_0(E)} \leq \|v\|_{H^1(E)} \leq \left(1 + K_E^2\right)^{1/2} \|v\|_{H^1_0(E)}. \tag{1.4}$$

Now consider a bounded domain $D \subset E \subset \mathbb{R}^2$. If $v \in H_0^1(E)$ then $v \in H^1(D)$ and clearly, $\|v\|_{H^1(D)} \leq \|v\|_{H^1(E)}$. Assuming $\partial D$ is sufficiently smooth, we can examine the trace of any $v \in H^1(E)$ on $\partial D$. Instead of the usual trace operator that relates $H^1(E)$ functions to their boundary values, we consider a trace operator

$$\tau : H^1(E) \to H^{1/2}(\partial D),$$

where $\partial D$ is a one-dimensional closed curve contained in $E$. In this setting, we define

$$H^{1/2}(\partial D) := \left\{\theta \,:\, \theta = \tau(v) \text{ for some } v \in H^1(E)\right\}, \tag{1.5}$$

the set of traces of $H^1(E)$ functions on $\partial D$, which is equipped with the norm

$$\|\theta\|_{H^{1/2}(\partial D)} := \inf_{v \in H^1(E), \tau(v)=\theta} ||v||_{H^1(E)}. \tag{1.6}$$

We identify $H^{-1/2}(\partial D)$ as the dual space of $H^{1/2}(\partial D)$ and if we define the duality pairing by

$$\langle \mu, \theta \rangle_{\partial D} := \int_{\partial D} \mu(s)\, \theta(s)\, ds, \qquad \mu \in H^{-1/2}(\partial D), \theta \in H^{1/2}(\partial D),$$

then the natural norm on $H^{-1/2}(\partial D)$ is given by

$$\|\mu\|_{H^{-1/2}(\partial D)} := \sup_{\theta \in H^{1/2}(\partial D)} \frac{\langle \mu, \theta \rangle_{\partial D}}{\|\theta\|_{H^{1/2}(\partial D)}}. \tag{1.7}$$

**2. FDM for deterministic problem.** Let $D \subset \mathbb{R}^2$ be a bounded polygon and consider the elliptic BVP: find $p : \overline{D} \to \mathbb{R}$ such that,

$$-\nabla \cdot (a(\boldsymbol{x}) \nabla p(\boldsymbol{x})) = f(\boldsymbol{x}), \qquad \text{in } D, \tag{2.1}$$

$$p(\boldsymbol{x}) = 0, \qquad \text{on } \partial D. \tag{2.2}$$

The BVP (2.1)–(2.2) is the deterministic analogue of (1.2)–(1.3) and we recall that the standard weak formulation is: find $p \in H_0^1(D)$ such that

$$\int_D a(\boldsymbol{x}) \nabla p(\boldsymbol{x}) \cdot \nabla v(\boldsymbol{x})\, d\boldsymbol{x} = \int_D f(\boldsymbol{x})\, v(\boldsymbol{x})\, d\boldsymbol{x}, \quad \forall v \in H_0^1(D). \tag{2.3}$$

In the deterministic case, the fictitious domain method (FDM) is advantageous when $D$ is difficult to mesh. Instead of solving (2.3), a "fictitious domain" $E$ with simple geometry is chosen with $\overline{D} \subset E \subset \mathbb{R}^2$. The weak problem is solved on $E$ and a Lagrange multiplier is used to constrain the solution so that (2.2) is satisfied weakly. We must hence assume that $f$ and $a$ can be extended to $E$ and, in particular, that $f \in L^2(E)$ and $a \in L^\infty(E)$ with $0 < a_{min} < a(\boldsymbol{x}) < a_{max}$ almost everywhere in $E$.

Define the Lagrangian function $\mathcal{L} : H_0^1(E) \times H^{-1/2}(\partial D) \to \mathbb{R}$ by

$$\mathcal{L}(v, \mu) := \frac{1}{2} \int_E a(\boldsymbol{x})\, |\nabla v(\boldsymbol{x})|^2\, d\boldsymbol{x} - \int_E f(\boldsymbol{x})\, v(\boldsymbol{x})\, d\boldsymbol{x} + \int_{\partial D} \mu(s)\, \tau(v)(s)\, ds, \tag{2.4}$$

where $\tau : H^1(E) \to H^{1/2}(\partial D)$ is the trace operator discussed in Section 1.1. We now consider the saddle point pair $(\widehat{p}, \lambda) \in H_0^1(E) \times H^{-1/2}(\partial D)$ satisfying

$$\inf_{v \in H_0^1(E)} \sup_{\mu \in H^{-1/2}(\partial D)} \mathcal{L}(v, \mu) \tag{2.5}$$

which can be found [8] by solving: find $(\widehat{p},\lambda) \in H_0^1(E) \times H^{-1/2}(\partial D)$ such that

$$\int_E a(\boldsymbol{x})\,\nabla\widehat{p}(\boldsymbol{x})\cdot\nabla v(\boldsymbol{x})\,d\boldsymbol{x} + \int_{\partial D}\lambda(s)\,\tau(v)(s)\,ds = \int_E f(\boldsymbol{x})\,v(\boldsymbol{x})\,d\boldsymbol{x}, \tag{2.6}$$

$$\int_{\partial D}\mu(s)\,\tau(\widehat{p})(s)\,ds = 0, \tag{2.7}$$

for all $v \in H_0^1(E)$ and $\mu \in H^{-1/2}(\partial D)$. Here, we apply homogeneous Dirichlet boundary conditions on $E$ but this is not a restriction. We note that $\widehat{p}|_D = p$, where $p$ solves (2.3) and $\lambda = [\partial\widehat{p}/\partial n]_{\partial D}$, the jump of the normal derivative of $\widehat{p}$ across $\partial D$; see [9].

THEOREM 2.1. *Let $a \in L^\infty(E)$ with $0 < a_{min} \le a(\boldsymbol{x}) \le a_{max}$ for almost all $\boldsymbol{x} \in E$ and $f \in L^2(E)$. Then (2.6)–(2.7) has a unique solution $(\widehat{p},\lambda) \in H_0^1(E) \times H^{-1/2}(\partial D)$.*

*Proof.* We appeal to the classical theory of saddle point problems [8], which states that a unique solution to (2.6)–(2.7) exists if the following conditions are satisfied.

1. $\exists c_1 > 0$ such that
$$\left|\int_E a(\boldsymbol{x})\nabla w(\boldsymbol{x})\cdot\nabla z(\boldsymbol{x})\,d\boldsymbol{x}\right| \le c_1||w||_{H_0^1(E)}||z||_{H_0^1(E)}, \quad \forall\, w,z \in H_0^1(E).$$
2. $\exists c_2 > 0$ such that, for all $(z,\mu) \in H_0^1(E)\times H^{-1/2}(\partial D)$,
$$\left|\int_{\partial D}\mu(s)\tau(z)(s)\,ds\right| \le c_2||\mu||_{H^{-1/2}(\partial D)}||z||_{H_0^1(E)}.$$
3. $\exists\alpha > 0$ such that
$$\int_E a(\boldsymbol{x})\,|\nabla z(\boldsymbol{x})|^2\,d\boldsymbol{x} \ge \alpha||z||_{H_0^1(E)}, \quad \forall\, z \in X_0,$$
where $X_0 := \{z \in H_0^1(E) : \langle\mu,\tau(z)\rangle_{\partial D} = 0,\ \forall\mu \in H^{-1/2}(\partial D)\}$.
4. $\exists\beta > 0$ such that
$$\sup_{z\in H_0^1(E),z\neq 0}\frac{\langle\mu,\,\tau(z)\rangle_{\partial D}}{||z||_{H_0^1(E)}} \ge \beta\,||\mu||_{H^{-1/2}(\partial D)}, \qquad \forall\mu \in H^{-1/2}(\partial D). \tag{2.8}$$

Using the assumption on $a$ and applying the Cauchy-Schwarz inequality we see that the first condition holds with $c_1 = a_{max}$. Using (1.6) and (1.4) gives

$$\begin{aligned}\left|\int_{\partial D}\mu(s)\tau(z)(s)\,ds\right| &\le ||\tau(z)||_{H^{1/2}(\partial D)}||\mu||_{H^{-1/2}(\partial D)} \le ||z||_{H^1(E)}||\mu||_{H^{-1/2}(\partial D)}\\ &\le (1+K_E^2)^{1/2}||z||_{H_0^1(E)}||\mu||_{H^{-1/2}(\partial D)}\end{aligned} \tag{2.9}$$

and hence condition 2 holds with $c_2 = (1+K_E^2)^{1/2}$. Condition 3 is satisfied with $\alpha = a_{min}$ for all $z \in H_0^1(E)$ (by the definition of $||\cdot||_{H_0^1(E)}$). That condition 4 (the so-called inf-sup condition) holds is well known, (e.g., see [14, Section 2], or [9]). ∎

**2.1. Finite Element Discretization.** We use a mixed finite element method to discretize (2.6)–(2.7). Specifically, we consider a piecewise bilinear approximation to $\widehat{p}$ and a piecewise constant approximation to $\lambda$. To do this, we introduce two meshes, one on $E$ and one on $\partial D$. We choose $E$ to be a rectangle (there is no restriction) and

construct a uniform mesh of square elements with characteristic edge length $h$. The $n_h$ interior vertices are denoted $\boldsymbol{x}_1, \ldots, \boldsymbol{x}_{n_h}$ and we define $X_h := \text{span}\{\phi_1, \ldots, \phi_{n_h}\} \subset H_0^1(E)$, where $\phi_i$ is the piecewise bilinear function on $E$ satisfying $\phi_i(\boldsymbol{x}_j) = \delta_{ij}$. Next, we partition the polygonal boundary $\partial D$ into $n_H$ disjoint straight line segments $\partial D_i$ and assume that for each $i$, $H \le |\partial D_i| \le cH$ for some $c < \infty$ where $H := \min_i |\partial D_i|$. We then define $Y_H := \text{span}\{\psi_1, \ldots, \psi_{n_H}\} \subset H^{-1/2}(\partial D)$ where $\psi_i = 1|_{\partial D_i}$ satisfies $\psi_i(\boldsymbol{x}) = 1$ if $\boldsymbol{x} \in \partial D_i$ and $\psi_i(\boldsymbol{x}) = 0$, otherwise.

Working in $X_h \times Y_H$, the finite-dimensional analogue of (2.6)–(2.7) is: find $(\widehat{p}_h, \lambda_H) \in X_h \times Y_H$ such that,

$$\int_E a(\boldsymbol{x}) \nabla \widehat{p}_h(\boldsymbol{x}) \cdot \nabla v(\boldsymbol{x})\, d\boldsymbol{x} + \int_{\partial D} \lambda_H(s)\, \tau(v)(s)\, ds = \int_E f(\boldsymbol{x}) v(\boldsymbol{x})\, d\boldsymbol{x}, \quad (2.10)$$

$$\int_{\partial D} \mu(s)\, \tau(\widehat{p}_h)(s)\, ds = 0, \quad (2.11)$$

for all $v \in X_h$ and $\mu \in Y_H$. To show that (2.10)–(2.11) is well-posed, we appeal again to classical saddle point theory, [8]. Conditions 1-3 (see Theorem 2.1) are satisfied on the finite-dimensional spaces since $X_h \subset H_0^1(E)$ and $Y_H \subset H^{-1/2}(\partial D)$. The inf-sup condition now reads: $\exists \beta > \beta_* > 0$ (with $\beta_*$ independent of $h$ and $H$) such that

$$\sup_{z_h \in X_h, z_h \neq 0} \frac{\langle \mu_H, \tau(z_h) \rangle_{\partial D}}{\|z_h\|_{H_0^1(E)}} \ge \beta \|\mu_H\|_{H^{-1/2}(\partial D)}, \quad \forall \mu_H \in Y_H. \quad (2.12)$$

The choice of the mesh parameters is crucial. In [14], (2.12) is shown to hold when piecewise linear triangular elements are used on $E$, provided $3 \le H/h \le L$, for a constant $L$. Hence, we require that each element $\partial D_i$ on $\partial D$ is of a comparable length to $h$ but larger by a factor of at least three. This ensures the dimension of $X_h$ is large enough compared to that of $Y_H$. To the best of the authors' knowledge, there is no such theoretical result for bilinear elements (also used in [9]). However, numerical evidence suggests that a similar result holds.

Define $A \in \mathbb{R}^{n_h \times n_h}$ and $B \in \mathbb{R}^{n_H \times n_h}$ by

$$A_{ij} := \int_E a(\boldsymbol{x})\, \nabla \phi_i(\boldsymbol{x}) \cdot \nabla \phi_j(\boldsymbol{x})\, d\boldsymbol{x}, \quad B_{kj} := \int_{\partial D} \psi_k(s) \tau(\phi_j)(\boldsymbol{x}(s))\, ds.$$

Then, (2.10)–(2.11) leads to a linear system of the form

$$\begin{pmatrix} A & B^T \\ B & 0 \end{pmatrix} \begin{pmatrix} \widehat{\mathbf{p}} \\ \boldsymbol{\lambda} \end{pmatrix} = \begin{pmatrix} \mathbf{f} \\ \mathbf{0} \end{pmatrix},$$

where $f_j = \int_E f(\boldsymbol{x}) \phi_j(\boldsymbol{x})\, d\boldsymbol{x}$. In addition, define $A_I$ as $A$ with $a(\boldsymbol{x}) = 1$. Then, for $z_h \in X_h$ and $\mu_H \in Y_H$, we have

$$\|z_h\|^2_{H_0^1(E)} = \boldsymbol{z}^T A_I \boldsymbol{z}, \qquad \langle \mu_H, \tau(z_h) \rangle_{\partial D} = \boldsymbol{\mu}^T B \boldsymbol{z},$$

where $\boldsymbol{z} \in \mathbb{R}^{n_h}$, $\boldsymbol{\mu} \in \mathbb{R}^{n_H}$ are the vectors of coefficients appearing in the expansions of $z_h$ and $\mu_H$, respectively. Now, if we can find a matrix $X \in \mathbb{R}^{n_H \times n_H}$ such that

$$\|\mu_H\|^2_{H^{-1/2}(\partial D)} = \boldsymbol{\mu}^T X \boldsymbol{\mu}, \quad (2.13)$$

then (2.12) may equivalently be written as

$$\beta^2\, \boldsymbol{\mu}^T X \boldsymbol{\mu} \le \max_{\boldsymbol{z} \in \mathbb{R}^{n_h}} \frac{\left(\boldsymbol{\mu}^T B \boldsymbol{z}\right)^2}{\boldsymbol{z}^T A_I \boldsymbol{z}} = \boldsymbol{\mu}^T B A_I^{-1} B^T \boldsymbol{\mu}, \qquad \forall \boldsymbol{\mu} \in \mathbb{R}^{n_H} \setminus \{\mathbf{0}\}. \quad (2.14)$$

Hence, $\beta^2$ is the smallest eigenvalue $\lambda_{min}$ in $BA_I^{-1}B^T\boldsymbol{\mu} = \lambda X\boldsymbol{\mu}$. The matrix $X$ is not easy to compute, however, as $\|\cdot\|_{H^{-1/2}(\partial D)}$ is defined by (1.7). In Section 4, we will construct an $X$ such that $\|\mu_H\|^2_{H^{-1/2}(\partial D)} \approx \boldsymbol{\mu}^T X\boldsymbol{\mu}$.

A priori error estimates for the mixed finite element method on triangular meshes of $E$ are established in [14]. Since the solution $\widehat{p}$ to (2.6) is singular in the vicinity of $\partial D$, only on a strict subset $D' \subset D$ (see [6]), do we obtain the bound

$$||\widehat{p} - \widehat{p}_h||_{H_0^1(D')} \leq ch^{1-\epsilon}||f||_{L^2(E)}, \qquad \forall \epsilon > 0.$$

On domains that contain $\partial D$, the $H_0^1$ norm of the error is (in the worst case) $\mathcal{O}(h^{1/2})$.

**3. FDM for stochastic problem.** We now consider (1.2)–(1.3) and make the standard assumption that $D$ depends on $M$ independent real-valued random variables $\xi_1, \ldots, \xi_M : \Omega \to \mathbb{R}$ so that $D(\omega) = D(\boldsymbol{\xi}(\omega))$ where $\boldsymbol{\xi} := (\xi_1, \ldots, \xi_M)$. Denote the joint density of $\boldsymbol{\xi}$ by $\rho$ and define $\Gamma := \boldsymbol{\xi}(\Omega) \subset \mathbb{R}^M$ so that $\boldsymbol{y} = \boldsymbol{\xi}(\omega) \in \Gamma$. We assume that each $\xi_k$ is bounded and focus on the uniform distribution. Hence, if $\xi_k \sim U(-\gamma_k, \gamma_k)$ for some $\gamma_k > 0$, then $\Gamma = [-\gamma_1, \gamma_1] \times \cdots \times [-\gamma_M, \gamma_M]$ and

$$\rho(\boldsymbol{y}) = \prod_{k=1}^{M} (2\gamma_k)^{-1} \quad \text{for } \boldsymbol{y} \in \Gamma, \qquad \rho(\boldsymbol{y}) = 0 \quad \text{for } \boldsymbol{y} \in \mathbb{R}^M \setminus \Gamma.$$

The BVP (1.2)–(1.3) can now be written in the equivalent parametric form: find $p : \left\{(\boldsymbol{x}, \boldsymbol{y}) : \boldsymbol{y} \in \Gamma, \boldsymbol{x} \in \overline{D(\boldsymbol{y})}\right\} \to \mathbb{R}$ such that for almost all $\boldsymbol{y} \in \Gamma$,

$$-\nabla \cdot (a(\boldsymbol{x})\nabla p(\boldsymbol{x}, \boldsymbol{y})) = f(\boldsymbol{x}) \qquad \text{in } D(\boldsymbol{y}), \tag{3.1}$$

$$p(\boldsymbol{x}, \boldsymbol{y}) = 0 \qquad \text{on } \partial D(\boldsymbol{y}). \tag{3.2}$$

To establish well-posedness of weak formulations and to perform analysis, the parameterization of the boundary in terms of $\boldsymbol{y} = (y_1, \ldots, y_M)$ requires some thought. Following [9], we assume that for each $\boldsymbol{y} \in \Gamma$, $\partial D(\boldsymbol{y})$ may be obtained from the boundary $\partial D_0$ of a reference polygon $D_0 \subset \mathbb{R}^2$, by applying a piecewise smooth invertible mapping $\gamma_0 : \partial D_0 \times \Gamma \to \mathbb{R}^2$. That is, we assume there exists a well-behaved mapping $\gamma_0$ such that for each $\boldsymbol{y} \in \Gamma$, $\partial D(\boldsymbol{y}) = \gamma_0(\partial D_0, \boldsymbol{y})$ and $\partial D_0 = \gamma_0^{-1}(\partial D(\boldsymbol{y}), \boldsymbol{y})$.

Let $E \subset \mathbb{R}^2$ be a domain such that $E \supset D(\boldsymbol{y})$ for almost every $\boldsymbol{y}$ in $\Gamma$ and define

$$L^2_\rho(\Gamma, H_0^1(E)) := \Big\{ v : E \times \Gamma \to \mathbb{R} : \int_\Gamma \rho(\boldsymbol{y})\, \|v(\cdot, \boldsymbol{y})\|^2_{H^1(E)}\, d\boldsymbol{y} < \infty,$$
$$\text{and } v(\cdot, \boldsymbol{y}) = 0 \text{ on } \partial E \text{ (in the sense of trace) } \forall \boldsymbol{y} \in \Gamma \Big\}.$$

The fictitious domain weak formulation of (3.1)–(3.2) is: find $\widehat{p} \in L^2_\rho(\Gamma; H_0^1(E))$ and $\lambda \in L^2_\rho(\Gamma; H^{-1/2}(\partial D))$ such that

$$\int_\Gamma \rho \int_E a\nabla\widehat{p} \cdot \nabla v\, d\boldsymbol{x}\, d\boldsymbol{y} + \int_\Gamma \rho \int_{\partial D(\boldsymbol{y})} \lambda\, \tau_{\boldsymbol{y}}(v)\, ds\, d\boldsymbol{y} = \int_\Gamma \rho \int_E f\, v\, d\boldsymbol{x}\, d\boldsymbol{y}, \tag{3.3}$$

$$\int_\Gamma \rho \int_{\partial D(\boldsymbol{y})} \mu\, \tau_{\boldsymbol{y}}(\widehat{p})\, ds\, d\boldsymbol{y} = 0, \tag{3.4}$$

for all $v \in L^2_\rho(\Gamma; H_0^1(E))$ and $\mu \in L^2_\rho(\Gamma; H^{-1/2}(\partial D))$, where the trace operator $\tau_{\boldsymbol{y}} : H^1(E) \to H^{1/2}(\partial D(\boldsymbol{y}))$. For brevity, we now drop the arguments in the integrands. Note that each of the boundary integrals in (3.3)–(3.4) can be transformed into an integral on $\partial D_0$ using $\gamma_0^{-1}$. This mapping also allows us to associate

$H^{-1/2}(\partial D(\boldsymbol{y}))$ functions with $H^{-1/2}(\partial D_0)$ functions. Hence, the meaning we give to $\mu \in L^2_\rho(\Gamma; H^{-1/2}(\partial D))$ (see [9]) is that the function $\mu_0 : \partial D_0 \times \Gamma$ satisfying

$$\int_{\partial D_0} \mu_0(\cdot, \boldsymbol{y}) v_0 \, ds = \int_{\partial D(\boldsymbol{y})} \mu(\cdot, \boldsymbol{y}) \, (v_0 \circ \gamma_0^{-1}(\cdot, \boldsymbol{y})) \, ds, \qquad \forall v_0 \in H^{1/2}(\partial D_0), \forall \boldsymbol{y} \in \Gamma,$$

belongs to $L^2_\rho(\Gamma, H^{-1/2}(\partial D_0))$, where

$$L^2_\rho(\Gamma, H^{-1/2}(\partial D_0)) := \left\{ \mu_0 : \partial D_0 \times \Gamma \to \mathbb{R} : \int_\Gamma \rho(\boldsymbol{y}) \, \|\mu_0(\cdot, \boldsymbol{y})\|^2_{H^{-1/2}(\partial D_0)} \, d\boldsymbol{y} < \infty \right\}.$$

Well-posedness of (3.3)–(3.4) is established in [9, Proposition 6.1] for the case $a \equiv 1$. By assuming that (2.8) holds for the deterministic problem associated with any fixed $\boldsymbol{y} \in \Gamma$, with a constant $\beta$ independent of $\boldsymbol{y}$, it can be shown that

$$\sup_{z \in L^2_\rho(\Gamma; H^1_0(E)), z \neq 0} \frac{\langle \mu, \tau_{\boldsymbol{y}}(z) \rangle_{\partial D}}{||z||_{L^2_\rho(\Gamma; H^1_0(E))}} \geq \beta \, ||\mu||_{L^2_\rho(\Gamma; H^{-1/2}(\partial D))}, \quad \forall \mu \in L^2_\rho(\Gamma; H^{-1/2}(\partial D)).$$

That is, the stochastic problem (3.3)–(3.4) is inf-sup stable. When $a \neq 1$, if the assumption on $a$ in Theorem 2.1 holds, then the problem is well-posed.

**3.1. SCMFEM discretization.** To derive a finite-dimensional problem, we apply a SCMFEM. That is, we combine collocation on $\Gamma$ with the mixed finite element discretization from Section 2.1. A continuous approximation on $\Gamma$ is then constructed by interpolation.

Let $\Xi := \{\boldsymbol{y}_1, \ldots, \boldsymbol{y}_{n_c}\} \subset \Gamma \subset \mathbb{R}^M$ be a chosen set of collocation points. In the SCMFEM approach, for each $\boldsymbol{y}_r \in \Xi$ we find $(\widehat{p}^r_h, \lambda^r_{H_r}) \in X_h \times Y_{H_r}$ that solves

$$\int_E a \nabla \widehat{p}^r_h \cdot \nabla v \, d\boldsymbol{x} + \int_{\partial D(\boldsymbol{y}_r)} \lambda^r_{H_r} \tau_r(v) \, ds = \int_E f v \, d\boldsymbol{x}, \qquad \forall v \in X_h, \tag{3.5}$$

$$\int_{\partial D(\boldsymbol{y}_r)} \mu \, \tau_r(\widehat{p}^r_h) \, d\boldsymbol{x} = 0, \qquad \forall \mu \in Y_{H_r}, \tag{3.6}$$

where $\tau_r : H^1(E) \to H^{1/2}(\partial D(\boldsymbol{y}_r))$ is the trace operator for $\partial D(\boldsymbol{y}_r)$. We assume that $E$ is a rectangle, construct a uniform mesh of rectangles with edge length $h$, and choose $X_h \subset H^1_0(E)$ to be the set of piecewise bilinear functions. For each $\boldsymbol{y}_r \in \Gamma$, we partition $\partial D(\boldsymbol{y}_r)$ into $n_{H_r}$ disjoint straight line segments $\partial D^r_i$ such that for each one, $H_r \leq |\partial D^r_i| \leq c H_r$ for some $c < \infty$, where

$$H_r := \min_i |\partial D^r_i|.$$

We then define $Y_{H_r} := \text{span}\{\psi^r_1, \ldots, \psi^r_{n_{H_r}}\} \subset H^{-1/2}(\partial D(\boldsymbol{y}_r))$ where $\psi^r_i = 1|_{\partial D^r_i}$ is the indicator function associated with the element $\partial D^r_i$. Hence, $Y_{H_r}$ contains piecewise constant functions on $\partial D(\boldsymbol{y}_r)$. Note that the dimension $n_{H_r}$ may be different for each collocation point $\boldsymbol{y}_r$ and the partitions are not uniform in general.

After solving each of the decoupled problems (3.5)–(3.6), we construct an approximation to $\widehat{p}$ on $E \times \Gamma$ via

$$\widehat{p}_{h,\Xi}(\boldsymbol{x}, \boldsymbol{y}) := \sum_{r=1}^{n_c} \widehat{p}^r_h(\boldsymbol{x}) \, L_r(\boldsymbol{y}), \qquad \boldsymbol{x} \in E, \boldsymbol{y} \in \Gamma \tag{3.7}$$

where $L_r$ is the Lagrange polynomial satisfying $L_r(\boldsymbol{y}_s) = \delta_{rs}$. Note that $\widehat{p}_h^r$ is a finite element approximation to $\widehat{p}(\cdot, \boldsymbol{y}_r)$, where $\widehat{p}$ solves (3.3)–(3.4). Similarly, $\lambda_{H_r}^r$ approximates $\lambda(\cdot, \boldsymbol{y}_r)$. Constructing an interpolant from the Lagrange multiplier approximations is not quite so straightforward as each one is defined on a different one-dimensional manifold. However, using $\gamma_{0,r}^{-1} := \gamma_0^{-1}(\cdot, \boldsymbol{y}_r)$ to map $\lambda_{H_r}^r$ onto the boundary of the reference domain $D_0$, we can form an approximation on $\partial D_0 \times \Gamma$ via

$$\lambda_{0,\Xi}(\boldsymbol{x}_0, \boldsymbol{y}) := \sum_{r=1}^{n_c} (\lambda_{H_r}^r \circ \gamma_{0,r})(\boldsymbol{x}_0)\, L_r(\boldsymbol{y}), \qquad \boldsymbol{x}_0 = \gamma_{0,r}^{-1}(\boldsymbol{x}) \in \partial D_0, \boldsymbol{y} \in \Gamma. \quad (3.8)$$

From (3.7), we have $\widehat{p}_{h,\Xi} \in X_h \otimes S_\Xi$ where $S_\Xi := \text{span}\{L_r(\boldsymbol{y}), \boldsymbol{y}_r \in \Xi\}$. $S_\Xi$ is a set of multivariate polynomials determined by the set $\Xi$. We choose $\Xi$ so that

$$S_\Xi \subset L^2_\rho(\Gamma) := \left\{ v : \Gamma \to \mathbb{R} : \int_\Gamma \rho(\boldsymbol{y}) v(\boldsymbol{y})^2 \, d\boldsymbol{y} < \infty \right\}.$$

This gives $X_h \otimes S_\Xi \subset L^2_\rho(\Gamma, H_0^1(E))$. In so-called *tensor* product schemes, $\Xi$ is the Cartesian product of $M$ sets of interpolation points on the intervals $\Gamma_k = \xi_k(\Omega)$. Possibilities include Clenshaw-Curtis and Gauss points. If $d_k + 1$ points are selected on $\Gamma_k$, so that the one-dimensional rule is exact for polynomials of degree $d_k$, then $n_c = |\Xi| = \prod_{k=1}^M (d_k + 1)$. This is intractable as $M \to \infty$ and *sparse grid* schemes (e.g., see [18]) are favoured when $M$ is large. For the applications we have in mind here, however, we do not anticipate the number of random variables to be large. Certainly, far fewer than the number of variables required to represent a spatially varying uncertain material coefficient. In our experiments we apply tensor product schemes because $M$ is small.

The notation $S_\Xi$ is used to stress that the set $\Xi$ is part of the discretization. For tensor product schemes, the polynomial degrees $d_1, \ldots, d_M$ determine $\Xi$ and so, like $H$ and $H_r$, are discretization parameters. To ensure existence and uniqueness of the SCMFEM solution, it is sufficient to show that each of the $n_c$ deterministic problems (3.5)–(3.6) is well-posed. In particular, we must ensure that (2.12) holds for each one. Since the mesh parameter $H_r$ can be different for each $\partial D(\boldsymbol{y}_r)$, care must be taken in implementation to ensure that for each $\boldsymbol{y}_r$, $3 \le H_r/h < L$, for some $L > 0$.

The authors of [9] focus on a related stochastic Galerkin mixed finite element method (SGMFEM). It is equivalent to a tensor product collocation scheme in the case where $d + 1$ points are chosen on each $\Gamma_k$, so that $n_c = (d + 1)^M$. It can be shown that when $f$ is sufficiently smooth (and $a \equiv 1$), then $\widehat{p}$ is Hölder continuous as a function of $\boldsymbol{y}$ on $E$ with some exponent $\gamma \in (0, 1]$. However, on $D^* = \cap_{\boldsymbol{y} \in \Gamma} D(\boldsymbol{y})$, $\widehat{p}$ is smoother. Based on the results for the SGMFEM studied in [9], if we choose $d_k = d$ points in each direction, we can only expect that

$$\| \widehat{p} - \widehat{p}_{h,\Xi} \|_{L^2_\rho(\Gamma, H_0^1(E))} = \mathcal{O}(h^{1/2}) + \mathcal{O}(d^{-\gamma/2}).$$

However, on some strict subset $D' \subset D^*$, we have

$$\| \widehat{p} - \widehat{p}_{h,\Xi} \|_{L^2_\rho(\Gamma, H_0^1(D'))} = \mathcal{O}(h) + \mathcal{O}(d^{-r/2}),$$

where $r \ge 1$ depends on the regularity of $f$.

**3.2. Numerical results.** To illustrate the SCMFEM scheme, we present results for a test problem. Consider (1.2)–(1.3) with $a = 1$, $f = 1$ and

$$D(\omega) = \{\boldsymbol{x} = (x_1, x_2) : -0.5 \le x_1 \le 0.5 + \xi_1(\omega), -0.5 \le x_2 \le 0.5 + \xi_2(\omega)\}$$

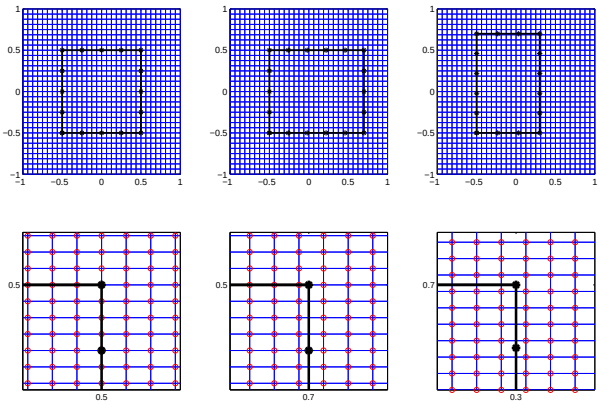

FIG. 3.1. *Top line: Uniform mesh on* $E = (-1,1)^2$ *with* $h = 1/16$ *and stable partitions of three sample boundaries* $\partial D(\boldsymbol{y}_r)$*, where* $D(\boldsymbol{y}_r) = (-0.5, 0.5 + y_{1,r}) \times (-0.5, 0.5 + y_{2,r})$*,* $r = 0, 1, 2$ *and* $\boldsymbol{y}_0 = (0,0)$*,* $H_0/h = 4$ *(left),* $\boldsymbol{y}_1 = (0.2, 0)$*,* $H_1/h = 3.84$ *(middle) and* $\boldsymbol{y}_2 = (-0.2, 0.2)$*,* $H_2/h = 3.84$ *(right). Bottom line: zoom of plots on top line.*

where $\xi_1 \sim U(-\gamma_1, \gamma_1)$ and $\xi_2 \sim U(-\gamma_2, \gamma_2)$ are independent, for some $\gamma_1, \gamma_2 > 0$. This corresponds to a rectangular domain of uncertain width and height with a fixed vertex at $(-0.5, -0.5)$. We choose $E = (-1,1)^2$ (note that it contains all realizations of $D$) and transform (1.2)–(1.3) into (3.3)–(3.4). We then perform collocation on $\Gamma = [-\gamma_1, \gamma_1] \times [-\gamma_2, \gamma_2]$ and apply the mixed finite element method from Section 3.1.

Each collocation point $\boldsymbol{y}_r \in \Gamma$ generates a new domain $D(\boldsymbol{y}_r)$ and a new saddle point system. Since $\partial D(\boldsymbol{y}_r)$ is one-dimensional, it is feasible to re-mesh it for each $\boldsymbol{y}_r$. For a fixed mesh on $E$ with elements of size $h$, we construct the mesh on $\partial D(\boldsymbol{y}_r)$ so that $|\partial D_i^r|/h$ is close to 4. Figure 3.1 shows a uniform mesh of squares on $E$ with $h = 1/16$ and three samples $D(\boldsymbol{y}_r)$ of $D$. The meshes constructed on the corresponding boundaries $\partial D(\boldsymbol{y}_r)$ are also shown. Observe that the number of elements on $\partial D(\boldsymbol{y}_r)$ varies with $\boldsymbol{y}_r$, and the meshes on $E$ and $\partial D(\boldsymbol{y}_r)$ are not necessarily aligned.

Now, let $\gamma_1 = 0.2 = \gamma_2$ and choose $\Xi = X_1 \times X_1$, where $X_1$ is the set of $d+1$ Gauss points in $[-0.2, 0.2]$. Cross-sections (at $x_2 = 0$) of the mean $\mathbb{E}[\widehat{p}_{h,\Xi}]$ and the variance $Var[\widehat{p}_{h,\Xi}]$ of the SCMFEM solution, obtained with $d = 26$ and varying choices of mesh parameters $h$ and $H_r$, are shown in Figure 3.2. There are 729 collocation points in total. To compute the statistics we set each $\widehat{p}_h(\cdot, \boldsymbol{y}_r)$ in (3.7) to zero in $E \backslash D(\boldsymbol{y}_r)$. As anticipated, there is little variation in the solution when $x_1 = -0.5$ and the largest variation occurs when $x_1 \approx 0.3$. A two-dimensional plot of the mean and variance of $\widehat{p}_{h,\Xi}$ obtained in the case $h = 1/64$ is also shown in Figure 3.3.

**4. Linear systems.** We now focus on the iterative solution of the sequence of linear systems corresponding to (3.5)–(3.6). We have to solve $n_c$ systems of the form

$$\underbrace{\begin{pmatrix} A & B_r^T \\ B_r & 0 \end{pmatrix}}_{=:C_r} \begin{pmatrix} \boldsymbol{p}_r \\ \boldsymbol{\lambda}_r \end{pmatrix} = \begin{pmatrix} \boldsymbol{b} \\ \boldsymbol{0} \end{pmatrix}, \qquad r = 1, \ldots, n_c, \tag{4.1}$$

where $n_c = |\Xi|$ is the number of collocation points. Note that the $r$th system consists of $n_h + n_{H_r}$ equations, where $n_h$ and $n_{H_r}$ are the dimensions of the spaces $X_h$ and

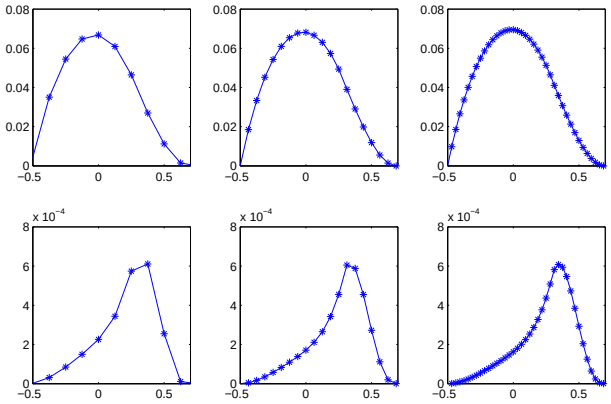

FIG. 3.2. *Cross-sectional plots on* $[-0.5, 0.7] \times \{0\}$ *of the expected SCMFEM solution* $\mathbb{E}[\widehat{p}_{h,\Xi}]$ *(top) and variance* $Var[\widehat{p}_{h,\Xi}]$ *(bottom) for the test problem with* $h = 1/8$ *(left),* $h = 1/16$ *(middle) and* $h = 1/32$ *(right). For all samples,* $3.6 \leq H_r/h \leq 4.4$*, for* $r = 1, \ldots, 729$*.*

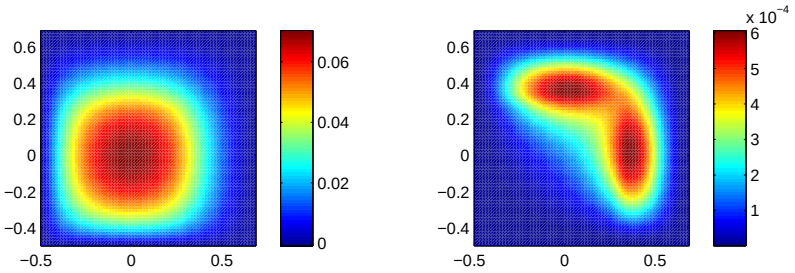

FIG. 3.3. *Plot of the expected SCMFEM solution* $\mathbb{E}[\widehat{p}_{h,\Xi}]$ *(left) and variance* $Var[\widehat{p}_{h,\Xi}]$ *(right) for the test problem with* $d = 26$*,* $h = 1/64$ *and* $3.9 \leq H_r/h \leq 4.1$*, for* $r = 1, \ldots, 729$*.*

$Y_{H_r}$, respectively. For each $r = 1, \ldots, n_c$,

$$[B_r]_{ij} = \int_{\partial D(\boldsymbol{y}_r)} \psi_i^r \tau_r(\phi_j)\, ds = \int_{\partial D_i^r} \phi_j|_{\partial D_i^r}\, ds, \tag{4.2}$$

for $i = 1, \ldots, n_{H_r}$, $j = 1, \ldots, n_h$, where $Y_{H_r} = \text{span}\{\psi_1^r, \ldots, \psi_{n_{H_r}}^r\}$ is the set of piecewise constant functions on $\partial D(\boldsymbol{y}_r)$. In addition, we have

$$A_{ij} = \int_E a(\boldsymbol{x}) \nabla\phi_i(\boldsymbol{x}) \cdot \nabla\phi_j(\boldsymbol{x})\, d\boldsymbol{x}, \qquad b_i = \int_E f(\boldsymbol{x})\phi_i(\boldsymbol{x})\, d\boldsymbol{x}, \quad i, j = 1, \ldots, n_h$$

where $X_h = \text{span}\{\phi_1, \ldots, \phi_{n_h}\} \subset H_0^1(E)$. We recognise $A$ as a standard finite element diffusion matrix; it is sparse, symmetric and positive definite. From (4.2) we see that the $(i, j)$th entry of $B_r$ is non-zero only when $\partial D_i^r$ intersects an element of $E$ with vertex $\boldsymbol{x}_j$ (where $\phi_j(\boldsymbol{x}_j) = 1$). Since $H_r/h$ is fixed to ensure stability, this number of elements is small relative to $n_h$ (see Figure 3.1), and hence $B_r$ is sparse.

Applying Sylvester's law of inertia reveals that the matrix $C_r$ in (4.1) has $n_h$ positive eigenvalues and $n_{H_r}$ negative eigenvalues. Consequently, it is indefinite as

well as symmetric and sparse. Linear systems with such coefficient matrices may be solved via the (preconditioned) minimal residual method (MINRES, see [20]) and this is the approach we take. Other authors (e.g., see [15]) have considered the iterative solution of the single linear system that arises when the FDM is applied to the deterministic problem (2.3). Instead of solving the indefinite system, however, existing studies focus on the reduced Schur-complement system associated with the Lagrange multiplier $\lambda$. This system has a dense positive definite matrix $BA^{-1}B^T$ (where $B$ is defined as in (4.2) but on a fixed domain). The authors of [15] discuss preconditioning for it, in the special case where $D$ is a circle.

To determine whether preconditioning is required when MINRES is used to solve the sequence of linear systems (4.1) associated with the stochastic PDE problem (1.2)–(1.3), we first examine eigenvalue bounds for the matrix $C_r$.

THEOREM 4.1. *Let $\theta, \Theta$ denote the minimum and maximum eigenvalues of $A$ and let $\sigma_{r,min}, \sigma_{r,max}$ be the minimum and maximum singular values of $B_r$. Then, for each $r = 1, \ldots, n_c$, the eigenvalues of $C_r$ in* (4.1) *are contained in*

$$\left[\frac{1}{2}\left(\theta - \sqrt{\theta^2 + 4\sigma_{r,max}^2}\right), \frac{1}{2}\left(\Theta - \sqrt{\Theta^2 + 4\sigma_{r,min}^2}\right)\right] \cup \left[\theta, \frac{1}{2}\left(\Theta + \sqrt{\Theta^2 + 4\sigma_{r,max}^2}\right)\right].$$

*Proof.* This is a well-known result, due to Rusten and Winther; see [22]. □

For bilinear elements on uniform meshes of $E$ and $a = 1$, it is known (e.g., see [11]) that the eigenvalues of $A$ are contained in a bounded interval of the form $[\, ch^2, \widehat{c}\,]$ for some $c, \widehat{c} > 0$, independent of $h$. Hence, $\theta = \mathcal{O}(h^2)$ and $\Theta = \mathcal{O}(1)$ in Theorem 4.1. If $a$ is spatially varying with $0 < a_{min} \leq a(\boldsymbol{x}) \leq a_{max}$ a.e. in $E$, then the eigenvalues of $A$ are contained in the interval

$$[\, ca_{min}h^2, a_{max}\widehat{c}\,].$$

The singular values of $B_r$, however, depend on the particular realization $\partial D(\boldsymbol{y}_r)$ and the associated mesh. The following simple example illustrates that $\sigma_{r,min}$ and $\sigma_{r,max}$ depend on both $h$ and $H_r$.

**Example 4.1** Consider $E = (-1, 1)^2$ and $D_0 = (-0.5, 0.5)^2 \subset E$. Since $D_0$ is square, we can partition $\partial D_0$ into $n_{H_0} = 4/H_0$ elements $\partial D_i^0$ of length $H_0$. On $E$, we select a uniform mesh of squares with edge length $h$. If $h = 2^{-k}$ for some $k \geq 1$, then the meshes on $E$ and $\partial D_0$ are aligned. For example, see the leftmost plot in Figure 3.1 (where $h = 1/16$ and $H_0 = 1/4$). Now, let $B_0$ be the rectangular matrix associated with $\partial D_0$, defined as in (4.2). We have

$$[B_0 B_0^T]_{ij} = \sum_{k=1}^{n_h} [B_0]_{ik}[B_0]_{jk}, \qquad i, j = 1, \ldots, n_{H_0},$$

and for the specific meshes described,

$$[B_0]_{ik} = \begin{cases} h & \text{if } \boldsymbol{x}_k \text{ lies in the interior of } \partial D_i^0 \\ h/2 & \text{if } \boldsymbol{x}_k \text{ is an end point of } \partial D_i^0 \\ 0 & \text{otherwise} \end{cases} \tag{4.3}$$

where $\boldsymbol{x}_k$ is a vertex of the mesh on $E$. Each $\partial D_i^0$ is composed of $H_0/h$ edges of elements in $E$. Hence, there are at most $H_0/h + 1$ nodes $\boldsymbol{x}_k$ such that $[B_0]_{ik}$ is non-zero. Two of these are end points of $\partial D_i^0$ and the rest lie in the interior. If $i = j$,

$$[B_0 B_0^T]_{ii} = \sum_{k=1}^{n_h} [B_0]_{ik}^2 = h^2/4 + h^2/4 + (H_0/h - 1)h^2 = h^2/2 + (H_0/h - 1)h^2,$$

and if $i \neq j$, then

$$[B_0 B_0^T]_{ij} = \sum_{k=1}^{n_h} [B_0]_{ik}[B_0]_{jk} = \begin{cases} h^2/4 & \text{if } \partial D_i^0 \text{ and } \partial D_j^0 \text{ are connected,} \\ 0 & \text{otherwise.} \end{cases} \tag{4.4}$$

If we number the elements $\partial D_i^0$ in a circular fashion, starting at the vertex $(-0.5, 0.5)$ and travelling around $\partial D_0$ in an anti-clockwise direction, it is easy to show that

$$B_0 B_0^T = \begin{pmatrix} (H_0 - h/2)h & h^2/4 & 0 & \dots & 0 & h^2/4 \\ h^2/4 & \ddots & \ddots & & \ddots & 0 \\ 0 & \ddots & \ddots & \ddots & 0 & \vdots \\ \vdots & 0 & \ddots & \ddots & \ddots & 0 \\ 0 & \ddots & & \ddots & \ddots & h^2/4 \\ h^2/4 & 0 & \dots & 0 & h^2/4 & (H_0 - h/2)h \end{pmatrix}. \tag{4.5}$$

The eigenvalues $\lambda_j$ of this symmetric circulant matrix are determined only by the entries in the first row (or column) and are given explicitly by

$$\lambda_j = [B_0 B_0^T]_{11} + [B_0 B_0^T]_{12}(\omega_{j-1} + \omega_{j-1}^{n_{H_0}-1}), \qquad j = 1, \dots, n_{H_0},$$

where $\omega_{j-1} = \exp(2\mathrm{i}\pi(j-1)/n_{H_0})$. The largest eigenvalue is

$$\lambda_1 = (H_0 - h/2)h + (h^2/4)(2) = H_0 h$$

and if $n_{H_0}$ is even, the smallest eigenvalue corresponds to $j = 1 + n_{H_0}/2$, which is

$$\lambda_{1+n_{H_0}/2} = (H_0 - h/2)h + (h^2/4)\left(\exp(\mathrm{i}\pi) + \exp(\mathrm{i}\pi)^{n_{H_0}-1}\right) = H_0 h - h^2.$$

Hence, the smallest and largest singular values of $B_0$ are, respectively,

$$\sigma_{0,min} = \sqrt{H_0 h - h^2}, \qquad \sigma_{0,max} = \sqrt{H_0 h}.$$

If we fix $H_0/h = L_0$, then $H_0 h = L_0 h^2$ and both $\sigma_{0,min}$ and $\sigma_{0,max}$ are $\mathcal{O}(h)$.

The above example tells us how the singular values of $B_r$ behave with respect to the mesh parameters, for *one* particular realization of the uncertain domain. For other realizations, the dependence of $\sigma_{r,min}$ and $\sigma_{r,max}$ in Theorem 4.1 on $H_r$ and $h$ varies with the relationship between the selected meshes on $\partial D(\boldsymbol{y}_r)$ and $E$.

**4.1. Preconditioning.** The discussion above tells us that for a fixed $\boldsymbol{y}_r$, the eigenvalues of $C_r$ in (4.1) depend on the mesh parameters $h$ and $H_r$ and the diffusion coefficient $a$. Since the eigenvalues depend on $\boldsymbol{y}_r$, the variation across all $n_c$ systems is potentially also affected by the standard deviation of the input random variables and by the polynomial degrees $d_k$ that determine the one-dimensional interpolation rules underpinning the tensor product collocation. Preconditioning is therefore essential. We consider block-diagonal preconditioners of the form

$$P_r = \begin{pmatrix} X_A & 0 \\ 0 & X_r \end{pmatrix}, \qquad r = 1, \dots, n_c, \tag{4.6}$$

where $X_A$ is a fixed symmetric and positive definite approximation to $A$ and $X_r$ is a symmetric and positive definite approximation to the Schur complement matrix

$$S_r := B_r A^{-1} B_r^T, \qquad r = 1, \dots, n_c. \tag{4.7}$$

REMARK 4.1. *SGMFEMs constructed using tensor product polynomial approximation in the variables $y_1, \ldots, y_M$ also lead to sequences of decoupled saddle point systems of the form* (4.1) *(see [9]). Hence, the preconditioners of the form* (4.6) *that we develop for SCMFEMs could also be applied for these alternative discretisations.*

The next result provides eigenvalue bounds for the preconditioned matrix $P_r^{-1}C_r$.

THEOREM 4.2. *Let $\theta$, $\Theta$ denote the minimum and maximum eigenvalues of $X_A^{-1}A$, respectively, and let $\alpha_r, \beta_r$ denote the minimum and maximum eigenvalues of $X_r^{-1}S_r$. Then, for each $r = 1, \ldots, n_c$, the eigenvalues $\lambda$ of*

$$\begin{pmatrix} A & B_r^T \\ B_r & 0 \end{pmatrix} \begin{pmatrix} \boldsymbol{u}_r \\ \boldsymbol{p}_r \end{pmatrix} = \lambda \begin{pmatrix} X_A & 0 \\ 0 & X_r \end{pmatrix} \begin{pmatrix} \boldsymbol{u}_r \\ \boldsymbol{p}_r \end{pmatrix}$$

*are contained in the union of two intervals*

$$\left[\frac{1}{2}\left(\theta - \sqrt{\theta^2 + 4\Theta\beta_r}\right), \frac{1}{2}\left(\Theta - \sqrt{\Theta^2 + 4\theta\alpha_r}\right)\right] \cup \left[\theta, \frac{1}{2}\left(\Theta + \sqrt{\Theta^2 + 4\Theta\beta_r}\right)\right].$$

*Proof.* The eigenvalues we seek coincide with those of

$$P_r^{-1/2} C_r P_r^{-1/2} = \begin{pmatrix} X_A^{-1/2} A X_A^{-1/2} & X_A^{-1/2} B_r^T X_r^{-1/2} \\ X_r^{-1/2} B_r X_A^{-1/2} & 0 \end{pmatrix} =: \begin{pmatrix} \tilde{A} & \tilde{B}_r^T \\ \tilde{B}_r & 0 \end{pmatrix}.$$

The eigenvalues of $\tilde{A}$ coincide with those of $X_A^{-1}A$ and the squares of the singular values of $\tilde{B}_r$ are the eigenvalues of $\tilde{B}_r\tilde{B}_r^T = X_r^{-1/2}\left(B_r X_A^{-1} B_r^T\right) X_r^{-1/2}$. Note that the latter coincide with the eigenvalues of $X_r^{-1}\left(B_r X_A^{-1} B_r^T\right)$. Now, since,

$$\frac{\boldsymbol{v}^T\left(B_r X_A^{-1} B_r^T\right)\boldsymbol{v}}{\boldsymbol{v}^T X_r \boldsymbol{v}} = \left(\frac{\boldsymbol{v}^T B_r X_A^{-1} B_r^T \boldsymbol{v}}{\boldsymbol{v}^T S_r \boldsymbol{v}}\right)\left(\frac{\boldsymbol{v}^T S_r \boldsymbol{v}}{\boldsymbol{v}^T X_r \boldsymbol{v}}\right), \qquad \forall \boldsymbol{v} \in \mathbb{R}^{n_{H_r}} \setminus \{\boldsymbol{0}\},$$

and the eigenvalues of $S_r^{-1}\left(B_r X_A^{-1} B_r^T\right)$ coincide with those of $X_A^{-1}A$, we conclude that the squares of the singular values of $\tilde{B}_r$ are contained in $[\theta\alpha_r, \Theta\beta_r]$. The result now follows by applying Theorem 4.1. ∎

To approximate the action of $A^{-1}$, we apply a V-cycle of algebraic multigrid (AMG, [7], [26], [27]) with symmetric smoothing. This implicitly defines the matrix $X_A$ that we will use in (4.6). Note that $A$ is an $M$-matrix (the meshes on $E$ are uniform) and for such matrices, AMG provides an optimal approximation. That is, the constants $\theta$ and $\Theta$ in the bounds in Theorem 4.2 are independent of $h$ and often insensitive to $a$. Many other efficient solvers for diffusion problems exist which can be used for $X_A$. The challenge in designing a good preconditioner $P_r$ of the form (4.6) lies in identifying a matrix $X_r$ such that the constants $\alpha_r$ and $\beta_r$ in the bounds in Theorem 4.2 are (ideally) independent of $h$ and $H_r$, for each $r$.

Consider, first, the linear operator $\mathcal{S}_r : H^{-1/2}(\partial D(\boldsymbol{y}_r)) \to H^{1/2}(\partial D(\boldsymbol{y}_r))$ defined by $\mathcal{S}_r\mu_r := \tau_r(u_{\mu_r})$, where $u_{\mu_r} \in H_0^1(E)$ satisfies

$$\int_E a\nabla u_{\mu_r} \cdot \nabla v \, d\boldsymbol{x} = \int_{\partial D(\boldsymbol{y}_r)} \mu_r \tau_r(v)\, ds, \qquad \forall v \in H_0^1(E)$$

and $\tau_r : H^1(E) \to H^{1/2}(\partial D(\boldsymbol{y}_r))$ is the trace operator. It follows that

$$\langle \mathcal{S}_r\mu_r, \mu_r\rangle_{\partial D(\boldsymbol{y}_r)} = s_r(\mu_r, \mu_r)$$

where $s_r : H^{-1/2}(\partial D(\boldsymbol{y}_r)) \times H^{-1/2}(\partial D(\boldsymbol{y}_r)) \to \mathbb{R}$ is defined by

$$s_r(\mu, \nu) := \int_E a \nabla u_\mu \cdot \nabla u_\nu \, d\boldsymbol{x}.$$

Since we assumed that $a$ is positive and bounded on $E$, the bilinear form $s_r(\cdot, \cdot)$ is symmetric, positive definite and $H^{-1/2}(\partial D(\boldsymbol{y}_r))$-elliptic; see [15, Proposition 3.1]. Hence, for any $\mu_r \in H^{-1/2}(\partial D(\boldsymbol{y}_r))$, we have

$$c_{1,r} \left\|\mu_r\right\|^2_{H^{-1/2}(\partial D(\boldsymbol{y}_r))} \leq \langle \mathcal{S}_r \mu_r, \mu_r \rangle_{\partial D(\boldsymbol{y}_r)} \leq c_{2,r} \left\|\mu_r\right\|^2_{H^{-1/2}(\partial D(\boldsymbol{y}_r))}, \tag{4.8}$$

for some $c_{1,r}, c_{2,r} > 0$ depending on $a$ and $r$ (due to the change in geometry).

Now consider the analogous operator $\widehat{\mathcal{S}}_r : Y_{H_r} \to Z_h^r$ associated with the finite-dimensional spaces $Y_{H_r} \subset H^{-1/2}(\partial D(\boldsymbol{y}_r))$ and $Z_h^r \subset H^{1/2}(\partial D(\boldsymbol{y}_r))$, where $Z_h^r := \tau_r(X_h)$ is the set of traces of piecewise bilinear functions on $E$. The Schur complement matrix $S_r$ in (4.7) is a discrete representation of this operator. Indeed, for $\mu_r \in Y_{H_r}$ we have $\widehat{\mathcal{S}}_r \mu_r := \tau_r(u_{\mu_r})$, where $u_{\mu_r} = \sum_{i=1}^{n_h} u_i \phi_i \in X_h$ satisfies,

$$\int_E a \nabla \left( \sum_{i=1}^{n_h} u_i \phi_i \right) \cdot \nabla \phi_j = \int_{\partial D(\boldsymbol{y}_r)} \mu_r \tau_r(\phi_j) \, ds, \qquad j = 1, \ldots, n_h.$$

Writing $\mu_r = \sum_{i=1}^{n_{H_r}} \mu_{r,i} \psi_i^r$ then gives

$$\sum_{i=1}^{n_h} u_i \left( \int_E a \nabla \phi_i \cdot \nabla \phi_j \, d\boldsymbol{x} \right) = \sum_{i=1}^{n_{H_r}} \mu_{r,i} \left( \int_{\partial D(\boldsymbol{y}_r)} \psi_i^r \tau_r(\phi_j) \, ds \right),$$

for $j = 1, \ldots, n_h$ and so $A \boldsymbol{u}_{\boldsymbol{\mu_r}} = B_r^T \boldsymbol{\mu}_r$ where $\boldsymbol{u}_{\boldsymbol{\mu_r}} = [u_1, \ldots, u_{n_h}]^T$ and $\boldsymbol{\mu}_r = [\mu_{r,1}, \ldots, \mu_{r,n_{H_r}}]^T$. Hence, for each $\mu_r \in Y_{H_r}$,

$$\begin{aligned} \left\langle \widehat{\mathcal{S}}_r \mu_r, \mu_r \right\rangle_{\partial D(\boldsymbol{y}_r)} &= \int_{\partial D(\boldsymbol{y}_r)} \mu_r \tau_r(u_{\mu_r}) \, ds = \int_E a \nabla u_{\mu_r} \cdot \nabla u_{\mu_r} \, d\boldsymbol{x} = \boldsymbol{u_{\mu_r}}^T A \boldsymbol{u_{\mu_r}} \\ &= (A^{-1} B_r^T \boldsymbol{\mu}_r)^T (B_r^T \boldsymbol{\mu}_r) = \boldsymbol{\mu}_r^T B_r A^{-1} B_r^T \boldsymbol{\mu}_r =: \boldsymbol{\mu}_r^T S_r \boldsymbol{\mu}_r. \end{aligned}$$

It also follows that

$$\left\langle \widehat{\mathcal{S}}_r \mu_r, \mu_r \right\rangle_{\partial D(\boldsymbol{y}_r)} = s_r(\mu_r, \mu_r), \qquad \forall \mu_r \in Y_{H_r},$$

and since $s_r(\cdot, \cdot)$ is $H^{-1/2}(\partial D(\boldsymbol{y}_r))$-elliptic and $Y_{H_r} \subset H^{-1/2}(\partial D(\boldsymbol{y}_r))$, we have

$$c_{1,r} \|\mu_r\|^2_{H^{-1/2}(\partial D(\boldsymbol{y}_r))} \leq \left\langle \widehat{\mathcal{S}}_r \mu_r, \mu_r \right\rangle_{\partial D(\boldsymbol{y}_r)} \leq c_{2,r} \|\mu_r\|^2_{H^{-1/2}(\partial D(\boldsymbol{y}_r))}, \qquad \forall \mu_r \in Y_{H_r}$$

where $c_{1,r}$ and $c_{2,r}$ are the positive constants from (4.8). Hence,

$$c_{1,r} \|\mu_r\|^2_{H^{-1/2}(\partial D(\boldsymbol{y}_r))} \leq \boldsymbol{\mu}_r^T S_r \boldsymbol{\mu}_r \leq c_{2,r} \|\mu_r\|^2_{H^{-1/2}(\partial D(\boldsymbol{y}_r))}, \qquad \forall \mu_r \in Y_{H_r}. \tag{4.9}$$

Now, if we can construct an $n_{H_r} \times n_{H_r}$ matrix $X_r$ that satisfies

$$b_{1,r} \|\mu_r\|^2_{H^{-1/2}(\partial D(\boldsymbol{y}_r))} \leq \boldsymbol{\mu}_r^T X_r \boldsymbol{\mu}_r \leq b_{2,r} \|\mu_r\|^2_{H^{-1/2}(\partial D(\boldsymbol{y}_r))}, \ \forall \mu_r \in Y_{H_r}, \tag{4.10}$$

for some positive constants $b_{1,r}$ and $b_{2,r}$, then we have

$$\frac{c_{1,r}}{b_{2,r}} \leq \frac{\boldsymbol{\mu}_r^T S_r \boldsymbol{\mu}_r}{\boldsymbol{\mu}_r^T X_r \boldsymbol{\mu}_r} \leq \frac{c_{2,r}}{b_{1,r}}. \tag{4.11}$$

If the action of $X_r^{-1}$ can be effected cheaply and $b_{1,r}$ and $b_{2,r}$ in (4.10) do not depend on $h$ or $H_r$, then (4.11) tells us that we have a good preconditioner for $S_r$. Since we have a sequence of systems to solve, it would be desirable to have bounds that are insensitive to the change in geometry induced by $\boldsymbol{y}_r$. It is unlikely that we can satisfy this in practice. Moreover, since $c_{1,r}$ and $c_{2,r}$ depend on $a_{min}$ and $a_{max}$, the bounds in (4.11) will be sensitive to the diffusion coefficient. Nevertheless, the above discussion does tells us that a sensible choice for $X_r$ is a matrix representation of a norm that is equivalent to $\|\cdot\|_{H^{-1/2}(\partial D(\boldsymbol{y}_r))}$.

Fractional power Sobolev spaces (e.g., $H^{-1/2}$, $H^{3/4}$) can be interpreted as interpolation spaces $[V, W]_\theta$, where $(V, W)$ is a generating pair of Hilbert spaces—with $V$ dense in $W$—and $\theta \in \mathbb{R}$ is the "index". Discrete representations of norms on such spaces are discussed in [1]. When the generating pair is a suitable pair of finite element spaces $V_h \subset V$, $W_h \subset W$ (of dimension $n$, say), it can be shown that the finite-dimensional interpolation space $[V_h, W_h]_\theta$ is equipped with a norm that is equivalent to the one on $[V, W]_\theta$. Matrix representations of the norm on $[V_h, W_h]_\theta$ are then readily constructed from $n \times n$ Grammian matrices associated with an appropriately chosen basis for $V_h$ and $W_h$. The authors of [1] apply this theory to construct a matrix representation of a norm that is equivalent to $\|\cdot\|_{H^{-1/2}(\partial D)}$ (where $\partial D \subset \mathbb{R}$ is the boundary of a fixed convex polygon). This is used to design a solver for the biharmonic problem. More precisely, $\partial D$ is first decomposed into edges $\Gamma_j$ (i.e., one-dimensional domains) and matrix representations of $\|\cdot\|_{H^{-1/2}(\Gamma_j)}$ are sought.

To develop a preconditioner $X_r$ for $S_r$, we follow [1] and assume that each realization $D(\boldsymbol{y}_r)$ of the uncertain domain is a convex polygon. Hence, we can decompose $\partial D(\boldsymbol{y}_r)$ into $K_r$ edges (straight lines), which we denote by $\Gamma_j^r \subset \mathbb{R}$. We do not consider circular domains. Then,

$$\partial D(\boldsymbol{y}_r) = \bigcup_{j=1}^{K_r} \Gamma_j^r, \qquad r = 1, \ldots, n_c$$

and we want to construct a matrix $X_r \in \mathbb{R}^{n_{H_r} \times n_{H_r}}$ of the form

$$X_r := \bigoplus_{j=1}^{K_r} X_r^j, \tag{4.12}$$

where $X_r^j$ is a discrete representation of a norm that is equivalent to $\|\cdot\|_{H^{-1/2}(\Gamma_j^r)}$.

Ideally, we want (4.10) to hold where, recall, $Y_{H_r}$ is the set of piecewise constant functions on $\partial D(\boldsymbol{y}_r)$. The analysis in [1] yields discrete representations of $\|\cdot\|_{H^{-1/2}(\Gamma_j^r)}$ on finite-dimensional subspaces of the dual space of

$$H_{00}^{1/2}(\Gamma_j^r) = [H_0^1(\Gamma_j^r), L^2(\Gamma_j^r)]_{1/2},$$

which is a subspace of $H^{-1/2}(\Gamma_j^r)$. To apply this analysis, however, we have to work with finite-dimensional subspaces $V_h$ of $V = H_0^1(\Gamma_j^r)$. This precludes the use of piecewise constant functions to construct $X_r^j$. Another difficulty is that $\Gamma_j^r$ is meshed independently of $E$ and (unlike the problems in [1]) does not inherit a mesh that is the restriction of the mesh on the domain of the underlying PDE problem. A natural idea is to use the traces of the bilinear basis functions $\phi_i$ for $X_h \subset H_0^1(E)$ to obtain a subspace of $H_0^1(\Gamma_j^r)$. However, since several $\phi_i$s have non-zero trace on each element of $\Gamma_j^r$, the dimension of the resulting subspace is too high.

We need a subspace of $H_0^1(\Gamma_j^r)$ of dimension $n_{j,r}$, where $n_{j,r}$ is the number of elements on $\Gamma_j^r$, so that $n_{1,r}+n_{2,r}+\cdots+n_{K_r,r} = n_{H_r} = \dim(Y_{H_r})$. We simply choose

$$V_{H_{j,r}} := \operatorname{span}\{\varphi_{1,j}^r, \ldots, \varphi_{n_{j,r},j}^r\} \subset H_0^1(\Gamma_j^r)$$

where $\varphi_{m,j}^r$ is a piecewise linear "hat function" associated with an interior vertex of a dual mesh on $\Gamma_j^r$ of width $H_{j,r} = |\Gamma_j^r| n_{j,r}^{-1}$. We then define $X_r^j \in \mathbb{R}^{n_{j,r}\times n_{j,r}}$ by

$$X_r^j := M_{j,r}(M_{j,r}^{-1}A_{j,r})^{-1/2}, \qquad j = 1, \ldots, K_r, \tag{4.13}$$

where $M_{j,r}$ and $A_{j,r}$ are mass and diffusion matrices associated with $\Gamma_i^r$. That is,

$$[M_{j,r}]_{mn} := \int_{\Gamma_j^r} \varphi_{m,j}^r(s)\, \varphi_{n,j}^r(s) ds, \qquad m, n = 1, \ldots, n_{j,r}, \tag{4.14}$$

$$[A_{j,r}]_{mn} := \int_{\Gamma_j^r} \frac{d\varphi_{m,j}^r(s)}{ds} \cdot \frac{d\varphi_{n,j}^r(s)}{ds}\, ds, \qquad m, n = 1, \ldots, n_{j,r}. \tag{4.15}$$

We have no rigourous proof about the dependence of the constants in (4.10) and (4.11) on $r$ and on the discretisation parameters. However, with the above construction, the theoretical arguments in [1] suggest that

$$b_{1,j}^r \|\mu_{j,r}\|_{H^{-1/2}(\Gamma_j^r)}^2 \le \boldsymbol{\mu}_{j,r}^T X_r^j \boldsymbol{\mu}_{j,r} \le b_{2,j}^r \|\mu_{j,r}\|_{H^{-1/2}(\Gamma_j^r)}^2, \qquad \forall \mu_{j,r} \in V_{H_{j,r}},$$

for some constants $b_{1,j}^r$ and $b_{2,j}^r$ depending on $j$ and here, on $r$, where $\boldsymbol{\mu}_{j,r}$ is the vector of coefficients associated with $\mu_{j,r}$ when expanded in the basis for $V_{H_{j,r}}$ and hence that (4.10) holds with $b_{1,r} = \min_j\{b_{1,j}^r\}$ and $b_{2,r} = \max_j\{b_{2,j}^r\}$ for functions

$$\mu_r \in V_{H_{1,r}} + V_{H_{2,r}} + \cdots + V_{H_{K_r,r}}.$$

Note that we do not fine-tune the choice of subspaces $V_{H_{j,r}}$ for the $r$th system and the dependence of the resulting constants $b_{1,j}^r$ and $b_{2,j}^r$ on $H_{j,r}$ and $r$ is not clear. However, our suggestion offers a fair compromise in terms of computational work. We simply construct two *one-dimensional* finite element matrices for each edge $\Gamma_j^r$. Given the mesh parameters $H_{j,r}$, $j = 1, \ldots, K_r$, this is computationally trivial. We could adapt the choice of $V_{H_{j,r}}$ to $\partial D(\boldsymbol{y}_r)$ more closely by working, say, with the traces of the basis functions for $X_h$ and then taking a linear interpolant with respect to the particular mesh on each $\Gamma_j^r$. This may result in improved bounds but requires more computational effort.

In summary, the matrix $X_r$ in (4.12) is the direct sum of matrices representing norms that are equivalent to the $H^{-1/2}$ norm on each edge $\Gamma_j^r$ of $\partial D(\boldsymbol{y}_r)$. Although we cannot specify the constants in (4.9) and (4.10), we do anticipate some variation in the performance of $X_r$ as a preconditioner for $S_r$, as $r$ varies. Moreover, since the norms do not incorporate the diffusion coefficient, the constants in the bounds in (4.9), and hence in (4.11), depend on $a$. When $a \neq 1$, some modification to $A_{j,r}$ and $M_{j,r}$ may be required to maintain robustness. We put this theory to the test for a simple model problem.

**4.2. Numerical results.** In this section, we report MINRES iteration counts obtained using the preconditioners

$$P_A = \begin{pmatrix} \text{AMG}(A) & 0 \\ 0 & I \end{pmatrix}, \qquad P_r = \begin{pmatrix} \text{AMG}(A) & 0 \\ 0 & X_r \end{pmatrix},$$

where AMG($A$) means that one V-cycle of AMG is applied to approximate the action of $A^{-1}$, $I$ is the $n_{H_r} \times n_{H_r}$ identity matrix and $X_r$ is defined in (4.12)–(4.13). Using $P_A$ constitutes a one-preconditioner-fits-all approach since it is fixed for all systems (up to the change in dimension of $I$). On the other hand, the preconditioner $P_r$ is different for each $r = 1, 2, \ldots, n_c$. Note that it is difficult to find *one* representative approximation for every matrix $S_r$, since the dimension changes with each sample of $\partial D(\boldsymbol{y})$. The usual 'mean-based' approach of constructing one preconditioner for all systems (e.g., see [12]), based on a fixed sample point such as $\boldsymbol{y}_0 = (0, 0)$, cannot be applied here.

In general, the cost of applying $n_c$ distinct preconditioners should not be overlooked. A few remarks are therefore warranted. Each preconditioned MINRES iteration with $P_r$ requires a matrix-vector multiplication with $X_r^{-1}$ and the application of one V-cycle of AMG to a linear system with coefficient matrix $A$. The latter can be performed optimally, in $\mathcal{O}(n_h)$ work. Note also that the AMG set-up only needs to be performed once, offline. Fortunately, $X_r$ is block-diagonal by construction and so

$$X_r^{-1} := \bigoplus_{j=1}^{K_r} \left(X_r^j\right)^{-1}, \quad \text{where} \quad (X_r^j)^{-1} = \left(M_{j,r}^{-1} A_{j,r}\right)^{1/2} M_{j,r}^{-1}. \tag{4.16}$$

Since diagonal approximations are efficient for mass matrices (e.g., see [28]) we also consider the following cheaper variants of $X_r$:

- $X_{r,diag}$ : defined as $X_r$ with the matrices $M_{j,r}$ replaced by their diagonals
- $X_{r,I}$ : defined as $X_r$ with the matrices $M_{j,r}$ replaced by identity matrices

leading to the following variants of the block-diagonal preconditioner $P_r$

$$P_{r,diag} = \begin{pmatrix} \text{AMG}(A) & 0 \\ 0 & X_{r,diag} \end{pmatrix}, \qquad P_{r,I} = \begin{pmatrix} \text{AMG}(A) & 0 \\ 0 & X_{r,I} \end{pmatrix}.$$

Applying the actions of $X_r^{-1}$, $X_{r,diag}^{-1}$ and $X_{r,I}^{-1}$ requires the computation of $K_r$ matrix square roots. This is not expensive since the dimensions of the matrices involved are equal to the numbers of elements on $\Gamma_j^r$, $j = 1, \ldots, K_r$, each of which is $\mathcal{O}(H_r^{-1})$. Recall also that $K$ is the number of sides of the convex polygon $D(\omega)$, and this is also small (e.g., $K_r = 4$ for a rectangle). Sophisticated methods for computing matrix square roots exist (e.g., see [1] and references therein), but are not needed here. In the experiments below, we simply use the MATLAB function `sqrtm`. For MINRES, we set the stopping tolerance on the preconditioned relative residual error to be $tol = 10^{-6}$.

**Test Problem 1** First, consider (1.2)–(1.3) with $a(\boldsymbol{x}) = 1$, $f(\boldsymbol{x}) = 1$ and

$$D(\omega) = \{\boldsymbol{x} = (x_1, x_2) : -0.5 \le x_1 \le 0.5 + \xi_1(\omega), -0.5 \le x_2 \le 0.5 + \xi_2(\omega)\}$$

where $\xi_1 \sim U(-\gamma_1, \gamma_1)$ and $\xi_2 \sim U(-\gamma_2, \gamma_2)$. The fictitious domain is chosen to be $E = (-1, 1)^2$ and we apply the FDM-SCMFEM scheme outlined in Section 3. We use a tensor product grid of collocation points $\boldsymbol{y}_r \in [-\gamma_1, \gamma_1] \times [-\gamma_2, \gamma_2]$, based on a $(d+1)$-point one-dimensional Gauss rule. This yields a sequence of $n_c = (d+1)^2$ saddle point systems of the form (4.1). The $K_r = 4$ edges of each sampled boundary $\partial D(\boldsymbol{y}_r)$ are partitioned such that the ratio $H_r/h$ is as close to 4 as possible.

In Table 4.1 we record the total number of MINRES iterations required to solve the single linear system (4.1) corresponding to the sample point $\boldsymbol{y}_0 = (0, 0)$. If we fix $H_0/h = 4$ then, with no preconditioner, the number of iterations required to satisfy the stated tolerance grows roughly like $h^{-3/2}$. When we apply the preconditioner

| Preconditioner | $h = 1/32$ $H_0 = 1/8$ | $h = 1/64$ $H_0 = 1/16$ | $h = 1/128$ $H_0 = 1/32$ | $h = 1/256$ $H_0 = 1/64$ |
|---|---|---|---|---|
| None | 112 | 295 | 732 | 1915 |
| $P_A$ | 22 | 39 | 51 | 62 |
| $P_0$ | 27 | 32 | 34 | 34 |
| $P_{0,diag}$ | 24 | 26 | 26 | 28 |
| $P_{0,I}$ | 18 | 22 | 22 | 23 |

TABLE 4.1

*Iteration counts for Test Problem 1 with $\gamma_1 = 0 = \gamma_2$, $d = 0$ (corresponding to one collocation point $\boldsymbol{y}_0 = (0, 0)$) and $H_0/h = 4$ fixed.*

$P_A$, the iteration counts grow less rapidly with mesh refinement but it is clear that convergence is not independent of the mesh parameters. All three variants of our new preconditioner $P_r$, however, are optimal! Iteration counts are completely independent of the discretization and are static as $h \to 0$ with $H_0/h$ fixed. The approximate preconditioner $P_{r,diag}$ leads to slightly lower iteration counts than $P_r$, because the chosen diagonal approximation to the mass matrix causes the eigenvalues of $X_{r,diag}^{-1} S_r$ to be more tightly clustered than those of $X_r^{-1} S_r$, and similarly for $P_{r,I}$.

Next, in Table 4.2, we record the average number and the range of MINRES iterations required to solve the entire sequence of $n_c = 121$ systems that arises when we select $\gamma_1 = 0.2 = \gamma_2$ and $d = 10$. We vary both $h$ and $H_r$ whilst keeping $H_r/h$ roughly fixed. The symbol $*$ indicates that the unpreconditioned experiment was too time-consuming to run. For each of the three variants of the preconditioner $P_r$, we observe that the minimum iteration count coincides with that obtained for the single linear system associated with $\boldsymbol{y}_0 = (0, 0)$ and is bounded as $h \to 0$. The maximum iteration count grows however, as $h \to 0$. This is slightly disappointing. However, it is to be expected that $P_r$ behaves differently for each system. There are several possible reasons for this. Some realizations of $\partial D(\boldsymbol{y})$ are roughly square and may be partitioned with uniform meshes, whereas some realizations are rectangular and necessarily have non-uniform meshes. In addition, the interplay between the meshes on $E$ and $\partial D(\boldsymbol{y}_r)$ changes. When $\boldsymbol{y}_0 = (0, 0)$, the meshes on $E$ and $\partial D(\boldsymbol{y}_0)$ happen to be aligned, and the preconditioner seems to work the best for that system. The choice of subspace $V_{H_{j,r}}$, which underpins the construction of the preconditioner, although optimal for some systems, is not the best possible one, for *all* systems.

The systems that have the highest preconditioned iteration counts also have the highest unpreconditioned iteration counts, suggesting that those systems are simply harder to solve. It is clear that $P_r$ does not perform well on some systems, for some values of $h$. However, when the entire sequence is considered collectively, the moderate increase in the *average* number of iterations as $h \to 0$ is acceptable. The most efficient preconditioner proved to be $P_{r,diag}$, which yielded a 98% decrease in the number of MINRES iterations compared to doing no preconditioning (in the case $h = 1/128$) and up to a 50% decrease compared to using the weaker preconditioner $P_A$ (for the range of values of $h$ considered).

To investigate the robustness of the preconditioners with respect to the stochastic discretization, we repeat the experiment reported on in Table 4.2, for $d = 26$. That is, we increase the degree of the polynomial for the Gauss rule that generates the set of collocation points. This yields $n_c = 729$ systems. Results are shown in Table 4.3. Comparing the iteration counts with those in Table 4.2, we see that the results are

| Preconditioner | $h = 1/32$ | $h = 1/64$ | $h = 1/128$ | $h = 1/256$ |
|---|---|---|---|---|
| None | 377 | 906 | 2062 | * |
| | [112, 445] | [295, 1033] | [732, 2331] | * |
| $P_A$ | 40 | 55 | 69 | 86 |
| | [22, 48] | [39, 61] | [51, 83] | [62, 101] |
| $P_r$ | 35 | 40 | 45 | 51 |
| | [27, 42] | [32, 54] | [34, 64] | [34, 108] |
| $P_{r,diag}$ | 30 | 34 | 38 | 43 |
| | [24, 34] | [26, 46] | [26, 52] | [28, 75] |
| $P_{r,I}$ | 30 | 35 | 42 | 48 |
| | [18, 37] | [22, 45] | [22, 56] | [23, 79] |

TABLE 4.2

*Average iteration counts and range $[min, max]$ for Test Problem 1 with $\gamma_1 = 0.2 = \gamma_2$, $d = 10$ ($n_c = 121$ systems) and varying $h$, $H_r$ with $3.6 < H_r/h < 4.4$.*

completely insensitive to the change in the discretization parameter $d$.

| Preconditioner | $h = 1/32$ | $h = 1/64$ | $h = 1/128$ | $h = 1/256$ |
|---|---|---|---|---|
| None | 391 | 917 | 2146 | * |
| | [112, 448] | [295, 1085] | [732, 2509] | * |
| $P_A$ | 41 | 54 | 70 | 88 |
| | [22, 48] | [39, 67] | [51, 85] | [62,109] |
| $P_r$ | 36 | 41 | 47 | 53 |
| | [27, 44] | [32, 64] | [34, 81] | [34, 110] |
| $P_{r,diag}$ | 30 | 34 | 40 | 44 |
| | [24, 38] | [26, 50] | [26, 67] | [28,80] |
| $P_{r,I}$ | 30 | 35 | 43 | 49 |
| | [18, 37] | [22, 51] | [22, 70] | [23, 91] |

TABLE 4.3

*Average iteration counts and range $[min, max]$ for Test Problem 1 with $\gamma_1 = 0.2 = \gamma_2$, $d = 26$ ($n_c = 729$ systems) and varying $h$, $H_r$ (keeping $3.6 < H_r/h < 4.4$).*

Finally, we vary the standard deviation of the two random variables that parameterize the uncertain boundary. Recall that $\xi_i \sim U(-\gamma_i, \gamma_i)$, $i = 1, 2$ and so the standard deviations are $\sigma_i = \gamma_i/\sqrt{3}$. Increasing $\sigma_i$ corresponds to increasing the amount of uncertainty we have in the geometry of the domain. We vary the standard deviation by varying $\gamma_1$ and $\gamma_2$. Results for $P_A$ and $P_{r,diag}$ are shown in Table 4.4, for $h$ fixed. Not only do we observe that both preconditioners are robust with respect to the standard deviation of $\xi_1$ and $\xi_2$, we also observe that the unpreconditioned iteration counts do not grow as the standard deviation increases. This suggests that the eigenvalues of the saddle point matrices $C_r$ are not affected directly by $\sigma_1$ and $\sigma_2$ but simply by the different meshes.

**Test Problem 2** We conclude by repeating Test Problem 1 with a non-unit diffusion coefficient. Specifically, we choose

$$a(\boldsymbol{x}) = \left(1 + 100(x_1^2 + x_2^2)\right)^{-1}, \tag{4.17}$$

which satisfies $a_{min} \leq a(\boldsymbol{x}) \leq a_{max}$ a.e. in $E = (-1, 1)^2$ with $a_{min} = \mathcal{O}(10^{-2})$ and $a_{max} = 1$. Iteration counts required to solve the single linear system associated with

| Preconditioner | $\gamma_1 = \gamma_2 = 0.1$ | $\gamma_1 = \gamma_2 = 0.2$ | $\gamma_1 = \gamma_2 = 0.4$ |
|---|---|---|---|
| None | 380 | 391 | 393 |
| | [112, 445] | [112, 448] | [112, 448] |
| $P_A$ | 39 | 41 | 40 |
| | [22, 48] | [22, 48] | [22, 48] |
| $P_{r,diag}$ | 29 | 30 | 30 |
| | [24, 36] | [24, 38] | [24, 38] |

TABLE 4.4

*Average iteration counts and range $[min, max]$ for Test Problem 1 with $d = 26$ ($n_c = 729$ systems), $h = 1/32$ and $3.6 < H_r/h < 4.4$, for varying $\gamma_1$ and $\gamma_2$.*

| Preconditioner | $h = 1/32$ $H_0 = 1/8$ | $h = 1/64$ $H_0 = 1/16$ | $h = 1/128$ $H_0 = 1/32$ | $h = 1/256$ $H_0 = 1/64$ | $h = 1/512$ $H_0 = 1/128$ |
|---|---|---|---|---|---|
| None | 509 | 1,476 | 4,051 | 10,962 | * |
| $P_A$ | 24 | 35 | 41 | 50 | 64 |
| $P_0$ | 41 | 47 | 53 | 57 | 62 |
| $P_{0,diag}$ | 33 | 37 | 41 | 45 | 49 |
| $P_{0,I}$ | 23 | 24 | 24 | 25 | 27 |

TABLE 4.5

*Iteration counts for Test Problem 2 with $\gamma_1 = 0 = \gamma_2$, $d = 0$ (corresponding to one collocation point $\boldsymbol{y}_0 = (0, 0)$) and $H_0/h = 4$ fixed.*

$\boldsymbol{y}_0 = (0, 0)$ are recorded in Table 4.5. Comparing with the results in Table 4.1, we observe that the unpreconditioned iteration counts have increased, confirming our hypothesis that the matrices $C_r$ are ill-conditioned with respect to $a$. We made no modification to $X_r$ to account for the non-unit coefficient, however, and we see that $P_r$ now fares worse than $P_A$ on all but one of the meshes considered. On very fine meshes, however, $P_r$ does start to yield lower iteration counts than $P_A$. The modified preconditioner $P_{r,diag}$ outperforms $P_A$ for the meshes with $h \leq 1/256$, while $P_{r,I}$ fares the best on all meshes.

| Preconditioner | $h = 1/32$ | $h = 1/64$ | $h = 1/128$ | $h = 1/256$ |
|---|---|---|---|---|
| $P_A$ | 41 | 50 | 62 | 78 |
| | [24, 54] | [35, 70] | [41, 93] | [50, 115] |
| $P_{r,diag}$ | 47 | 57 | 67 | 75 |
| | [33, 62] | [37, 76] | [41, 102] | [45, 132] |
| $P_{r,I}$ | 35 | 37 | 42 | 50 |
| | [23, 50] | [24, 54] | [24, 69] | [25, 89] |

TABLE 4.6

*Average iteration counts and range $[min, max]$ for Test Problem 2 with $\gamma_1 = 0.2 = \gamma_2$, $d = 26$ ($n_c = 729$ systems) and varying $h$, $H_r$ (keeping $3.6 < H_r/h < 4.4$).*

Next, in Table 4.6, we record the average number and the range of MINRES iterations required to solve the entire sequence of $n_c = 729$ systems that arises when we select $\gamma_1 = 0.2 = \gamma_2$ and $d = 26$. We vary both $h$ and $H_r$ whilst keeping $H_r/h$ close to 4. For brevity, we include only the results for the more efficient variants of the preconditioner. Comparing the results with those in Table 4.3 we see that once again, average preconditioned iteration counts increase slightly with mesh refinement. To

| Preconditioner | $\gamma_1 = \gamma_2 = 0.1$ | $\gamma_1 = \gamma_2 = 0.2$ | $\gamma_1 = \gamma_2 = 0.4$ |
|---|---|---|---|
| $P_A$ | 38 | 41 | 50 |
| | $[24, 46]$ | $[24, 54]$ | $[24, 77]$ |
| $P_{r,diag}$ | 41 | 47 | 57 |
| | $[33, 50]$ | $[33, 62]$ | $[33, 80]$ |
| $P_{r,I}$ | 31 | 35 | 44 |
| | $[23, 38]$ | $[23, 50]$ | $[23, 69]$ |

TABLE 4.7

*Average iteration counts and range $[min, max]$ for Test Problem 2 with $d = 26$ ($n_c = 729$ systems), $h = 1/32$ and $3.6 < H_r/h < 4.4$, for varying $\gamma_1$ and $\gamma_2$.*

combat this, some modification to $X_r$ would be required to account for the variation in $a(\boldsymbol{x})$ on $\partial D(\boldsymbol{y}_r)$. However, since this would have to be done for *each* $\boldsymbol{y}_r$, this increases computational costs. Recall, the constants $c_{1,r}$ and $c_{2,r}$ in the bounds (4.9) do depend on $a_{min}$ and $a_{max}$ in a potentially different manner, for each $r$. For $P_{r,I}$, however, the rise is acceptably small. In fact, only this version of the preconditioner beats $P_A$ on all the meshed considered.

Finally, we vary the standard deviations $\sigma_1, \sigma_2$ of the random variables $\xi_1$ and $\xi_2$. Comparing the results in Table 4.7 with those in Table 4.4 we see that increasing the standard deviations causes the average iteration counts to rise slightly. In contrast to the experiment with unit coefficients, the worst recorded performance of the preconditioner on a single system deteriorates as $\sigma_1, \sigma_2$ increase. When the standard deviations are increased, we encounter domains $D(\boldsymbol{y}_r)$ whose boundaries $\partial D(\boldsymbol{y}_r)$ are located in regions of E where $a(\boldsymbol{x})$ takes larger values. Since $X_r$ represents a norm that does not contain the diffusion coefficient, its performance is poorer for Schur-complements associated with these domains. For the specific coefficient (4.17), $a(\boldsymbol{x})$ takes is maximum value at the centre of $E$ and decays towards $\partial E$. Note also that $\boldsymbol{y}_0 = (0, 0)$ is a collocation point for any value of $\gamma_1$ and $\gamma_2$ and, in particular, $a(\boldsymbol{x})$ is small on the reference boundary $\partial D(\boldsymbol{y}_0)$ of $D(\boldsymbol{y}_0) = (-0.5, 0.5)^2$. The preconditioner performs best for that system, in particular.

**4.3. Conclusions.** We have demonstrated that the sequence of linear systems (4.1) arising from stochastic collocation mixed finite element discretizations of fictitious domain formulations of elliptic PDEs on uncertain parameterized domains can be solved efficiently using preconditioned MINRES. Although not optimal for each individual saddle point system, our novel block-diagonal preconditioner—which is based on a discrete approximation of the $H^{-1/2}$ norm on edgewise decompositions of the sampled boundaries $\partial D(\boldsymbol{y}_r)$—is practical and yields iteration counts that are robust with respect to the statistical parameters. Moreover, average iteration counts display only a slight growth with respect to spatial mesh refinement. A subset of the saddle point systems proved to be very challenging to solve and fine-tuning the preconditioner for this subset, to reduce average iteration counts even further, will be the subject of future work.

Since the only source of uncertainty in our model problem is in the domain geometry, only the off-diagonal block $B_r$ of the coefficient matrix $C_r$ in (4.1) changes from system to system. Incorporating multiple sources of data uncertainty into the underlying PDE model is our long-term goal and leads to saddle point systems in which more components change as the collocation point is varied. Of particular interest is

the elliptic BVP: find $p : \left\{(\boldsymbol{x},\omega) : \omega \in \Omega, \boldsymbol{x} \in \overline{D(\omega)}\right\} \to \mathbb{R}$ such that $\mathbb{P}-$a.s.,

$$\begin{aligned} -\nabla \cdot a(\boldsymbol{x},\omega)\nabla p(\boldsymbol{x},\omega) &= f(\boldsymbol{x}), \qquad \text{in } D(\omega)\times\Omega, \\ p(\boldsymbol{x},\omega) &= 0, \qquad \text{on } \partial D(\omega)\times\Omega. \end{aligned} \tag{4.18}$$

This arises in potential flow models where both the diffusion coefficient *and* the domain are uncertain. SCMFEM discretizations lead to very long sequences of saddle point matrices where both the $(1,1)$ block $A$ and the off-diagonal block $B$ change. We anticipate that combining the recycled AMG preconditioning strategy in [16] (for elliptic PDEs with uncertain coefficients on certain domains) and the $H^{-1/2}(\partial D(\boldsymbol{y}_r))$ preconditioner suggested in this work will yield an efficient solver for FDM-SCMFEM discretizations of (4.18).

## REFERENCES


[1] M. Arioli and D. Loghin, *Discrete interpolation norms with applications*, SIAM J. Numer. Anal., 47 (2009), pp. 2924–2951.

[2] K. Atkinson and W. Han, *Theoretical Numerical Analysis (2nd ed.)*, Springer-Verlag, New York, 2007.

[3] I. Babuska and J. Chleboun, *Effects of uncertainties in the domain on the solution of neumann boundary value problems in two spatial dimensions*, Math. Comput, 71 (1999), pp. 1339–1370.

[4] I. Babuška, F. Nobile, and R. Tempone, *A stochastic collocation method for elliptic partial differential equations with random input data*, SIAM J. Numer. Anal., 45 (2007), pp. 1005–1034.

[5] I. Babuška, R. Tempone, and G. E. Zouraris, *Galerkin finite element approximations of stochastic elliptic partial differential equations*, SIAM J. Numer. Anal., 42 (2004), pp. 800–825.

[6] S. Bertoluzza, *Interior estimates for the wavelet Galerkin method*, Numer. Math., 78 (1997), pp. 1–20.

[7] J. Boyle, M.D. Mihajlović, and J.A. Scott, *HSL_MI20: an efficient AMG preconditioner*. Technical Report RAL-TR-2007-021, SFTC Rutherford Appleton Laboratory, Didcot (2007).

[8] F. Brezzi and M. Fortin, *Mixed and Hybrid Finite Element Methods*, Springer-Verlag, New York, 1991.

[9] C. Canuto and T. Kozubek, *A fictitious domain approach to the numerical solution of PDEs in stochastic domains*, Numer. Math., 107 (2007), pp. 257–293.

[10] M. K. Deb, I. M. Babuška, and J. T. Oden, *Solution of stochastic partial differential equations using Galerkin finite element techniques*, Comput. Methods Appl. Mech. Engrg., 190 (2001), pp. 6359–6372.

[11] H. Elman, D. Silvester, and A. Wathen, *Finite Elements and Fast Iterative Solvers*, Oxford University Press, New York, 2005.

[12] O.G. Ernst, C.E. Powell, D.J. Silvester, and E. Ullmann, *Efficient solvers for a linear stochastic Galerkin mixed formulation of diffusion problems with random data*, SIAM J. Sci. Comput., 31 (2009), pp. 1424–1447.

[13] P. Frauenfelder, C. Schwab, and R. A. Todor, *Finite elements for elliptic problems with stochastic coefficients*, Comput. Methods Appl. Mech. Engrg., 194 (2005), pp. 205–228.

[14] V. Girault and R. Glowinski, *Error analysis of a fictitious domain method applied to a Dirichlet problem*, Japan J. Indust. Appl. Math., 12 (1995), pp. 487–514.

[15] R. Glowinski, T. Pan, and J Périaux, *A fictitious domain method for Dirichlet problems and applications*, Comput. Methods Appl. Mech. Engrg., 111 (1994), pp. 283–303.

[16] A.D. Gordon and C.E. Powell, *On solving stochastic collocation systems with algebraic multigrid*, IMA J. Numer. Anal., 32 (2012), pp. 1051–1070.

[17] A. Keese, *A review of recent developments in the numerical solution of stochastic partial differential equations (stochastic finite elements)*, Technical Report 2003–06, Institute of Scientific Computing, TU Braunschweig, 2003.

[18] F. Nobile, R. Tempone, and C. G. Webster, *A sparse grid stochastic collocation method for partial differential equations with random input data*, SIAM J. Numer. Anal., 46 (5) (2008), pp. 2309–2345.

[19] A. Nouy, M. Chevreuil, and E. Safatly, *Fictitious domain method and separated representations for the solution of boundary value problems on uncertain parameterized domains*, Comput. Methods Appl. Mech. Engrg., 200 (2011), pp. 3066–3082.
[20] C. C. Paige and M. A. Saunders, *Solutions of sparse indefinite systems of linear equations*, SIAM J. Numer. Anal., 12 (1975), pp. 617–629.
[21] C. Powell and H. Elman, *Block-diagonal preconditioning for spectral stochastic finite element systems*, IMA J. Numer. Anal., 29 (2009), pp. 350–375.
[22] T. Rusten and R. Winther, *A preconditioned iterative method for saddle point problems*, SIAM J. Matrix Anal. Appl., 13 (3) (1992), pp. 887–904.
[23] C. Schwab and R. Todor, *Sparse finite elements for elliptic problems with stochastic loading*, Numer. Math., 95 (2003), pp. 707–734.
[24] I. Babuška and P. Chatzipantelidis, *On solving elliptic stochastic partial differential equations*, Comput. Methods Appl. Mech. Engrg., 191 (2002), pp. 4093–4122.
[25] I. Babuška, F. Nobile, and R. Tempone, *A stochastic collocation method for elliptic partial differential equations with random input data*, SIAM J. Sci. Comput., 45 (3) (2007), pp. 1005–1034.
[26] K. Stüben, *A review of algebraic multigrid*, J. Comput. Appl. Math., 128 (2001), pp. 281–309.
[27] U. Trottenberg, C.W. Oosterlee, and A. Schüller, *Multigrid*, Academic Press, London, 2001.
[28] A. Wathen, *Realistic eigenvalue bounds for the Galerkin mass matrix*, IMA J. Numer. Anal., 7 (1987), pp. 449–457.
[29] D. Xiu and J. Hesthaven, *High-order collocation methods for differential equations with random inputs*, SIAM J. Sci. Comput., 27(3) (2005), pp. 1118–1139.
[30] D. Xiu and D.M. Tartakovsky, *Numerical methods for differential equations in random domains*, SIAM J. Sci. Comput., 28 (2006), pp. 1167–1185.